# The Potential of Microwave Communication Networks to Detect Dew—Experimental Study

Oz Harel, Noam David, Pinhas Alpert, and Hagit Messer, *Fellow, IEEE*

***Abstract*—At microwave frequencies of tens of GHz, various hydrometeors cause attenuations to the electromagnetic signals. Here, we focus on the effect of liquid water films accumulating on the outer coverage of the microwave units during times of high relative humidity (RH). We propose a novel technique to detect moist antenna losses using standard received signal level (RSL) measurements acquired simultaneously by multiple commercial microwave links (MLs). We use the generalized likelihood ratio test (GLRT) for detecting a transient signal of unknown arrival time and duration. The detection procedure is applied on real RSL measurements taken from an already existing microwave network. It is shown that moist antenna episodes can be detected, information which provides the potential to identify dew, an important hydro-ecological parameter.**

***Index Terms*—Attenuation, commercial microwave links (MLs), dew, generalized likelihood ratio test (GLRT), received signal level (RSL).**

## I. Introduction

YEARS of research have developed the capacity for modeling, understanding and mitigation of atmosphere-induced reductions of the quality of wireless communication links. After exposing the idea of using measurements from commercial cellular operators for rainfall monitoring [1], [2], this field of research has been extensively studied and developed [3]–[9]. Notably, nearly all of the research in this field has focused on rainfall monitoring.

However, rain is not the only source for impairments to the received radio signals. In the presence of a clear line of sight, such propagation phenomena—diffraction, refraction, absorption, and scattering—may cause acute reductions. At frequencies above 10 GHz, some of them (absorption and scattering) are directly related to other atmospheric phenomena. Thus, it has also been shown that microwave links (MLs) have the potential to monitor phenomena aside from rain, such as areal evaporation [10], water vapor density [11]–[13], and even fog [14], [15].

Excess attenuation due to antenna wetting during rainfall episodes has been studied [5], [10], [16]. However, until now, this effect has been considered as a negative perturbation, causing additional attenuations to the radio signals and thus interfering with the ability to conduct accurate rain rate measurements. However, in some cases, this perturbation contains vital information, particularly during times of dew: whenever condensation rate exceeds evaporation rate, a thin layer of water droplets accumulates directly on the antenna surface or the external radome, causing moistening of the radio units. This water film may lead to a signal loss, which can be measured by the microwave system. This effect has been recently shown to cause additional losses to the microwave signals during heavy fog events [14]. At an earlier stage, Hening and Stanton [17] measured experimentally the microwave attenuation caused by dew using a parabolic reflector antenna. The experiment was conducted when a dew layer was known to be present on the antenna reflector. Then, the water layer was wiped off the antenna at a certain known time. As a result, the signal level at 20 and 27 GHz channels gained 0.5 and 1.5 dB, respectively, immediately after the dew layer was removed.

According to the American Meteorological Society (AMS), dew is defined as water condensed onto grass and other objects at ground level while the temperature of which have fallen below the dew-point of the surface air due to radiational cooling during night time [18].

The motivation for monitoring this phenomenon rises from various ecological aspects. Dew can serve as an important source of moisture for animals [19], [20] and biological crusts that can contribute to the stabilization of sand dunes [21], [22]. Terrestrial microwave radiation is sensitive to soil moisture, which is an important element of the hydrological cycle, and affects weather and climate [23]. By observing terrestrial microwave emission, satellites can map soil moisture variability spatially and temporally [24]. However, terrestrial microwave emission is also affected by water in vegetation as dew (or intercepted precipitation). As a result, bias caused by the presence of free water can introduce error to the soil moisture measurement [25]–[28]. Therefore, high spatio-temporal information about dew, if obtained, can potentially be used in combination with remote sensing satellites to improve the ability to derive more accurate observations of soil moisture [28].

The perspective regarding the dew-plants interaction is controversial: plant pathologists emphasize the negative role played by dew in the promotion of plant diseases [29]. This being the case, agricultural warning systems of plant diseases, that assist growers in deciding on the appropriate time to use preventative measures, use information concerning the duration of leaf wetness as an input [30]. On the other hand, it has been found recently that dew formation serves as an integral part in the

Manuscript received December 26, 2014; revised July 02, 2015; accepted July 25, 2015.

O. Harel and H. Messer are with the School of Electrical Engineering, Tel Aviv University, Tel Aviv, Israel (e-mail: ozharel@gmail.com; messer@eng.tau.ac.il).

N. David is with the School of Civil and Environmental Engineering, Cornell University, Ithaca, NY USA (e-mail: nd363@cornell.edu).

P. Alpert is with the Department of Geosciences, Tel Aviv University, Tel Aviv, Israel (e-mail: pinhas@post.tau.ac.il).

Color versions of one or more of the figures in this paper are available online at http://ieeexplore.ieee.org.

Digital Object Identifier 10.1109/JSTARS.2015.2465909

general strategy of vegetation water economy in the arid and semiarid zones [31]. However, the information regarding dew in the literature is scarce, in part due to the difficulty associated with its measurement [32], [33]. Thus, standard meteorological stations do not measure this parameter, and other facilities have limited applications.

Typical dew detection and measuring instruments include drosometers and the leaf wetness sensors (LWSs). The drosometer is a large surface comprised of fine fiber (wool, cotton) or metal plate. It measures the amount of accumulating dew per unit area per time. The measurements are made in the early morning, before the rising sun evaporates the dew. However, these observations are considered inaccurate, primarily since the slightest change in the surface that receives the moisture alters the quantity of dew that is caught. The LWS is an apparatus used for identifying leaf wetness (i.e., dew). The operating principle of this device is based on a simple electronic circuit, which is completed when water bridges two inter digitated electrodes. It measures the fraction of time that moisture accumulates and completes the electronic circuit.

The goal of this paper is to address the problem of identifying antenna wetting periods during dew episodes utilizing received signal level (RSL) measurements from a spatially distributed MLs network. A novel method to detect moist antenna attenuation periods is suggested based on *signal detection theory* [34]. The extremely high density of ML [1], [35], which can reach several tens of links deployed over a single square km, especially in urban areas [14], guarantees markedly higher coverage when compared to any other sensor system, or the spatial coverage achieved by dew gauges deployed in conventional ground stations.

Let us briefly specify the different signal processing stages. First, we extract the physical characteristics of the meteorological phenomena observed. Accordingly, the meteorological phenomena induced attenuation can be formulated as an unknown deterministic signal and respectively the classical binary hypothesis testing problem (signal detection problem) is defined, where we aim to detect an unknown deterministic signal embedded in the interference signal. Second, we use the generalized likelihood ratio test (GLRT) [36] in order to discriminate the moist antenna attenuation from other atmospheric impairments. Finally, we apply the suggested method on real RSL measurements taken from an already existing microwave network.

The performance of the proposed method is quantified by an experimental receiver operating characteristics (ROC) curve where the validation process is conducted using LWS and relative humidity (RH) data taken from standard meteorological stations.

## II. Model and Method

### A. Model

Environmental monitoring techniques, like other signal processing systems such as Radar and Communication, share the basic goal of being able to detect whether an event of interest occurred (e.g., rainfall and fog) and then extract information concerning the event. The former task, of decision-making, is usually termed *detection theory*. The degree of difficulty of these problems is directly related to the information concerning the signal and noise characteristics which can be modeled in terms of their probability density functions (pdfs). Accordingly, let us define the detection model and the effects of humidity and dew on a ML as unknown deterministic attenuation signals.

A simplified model for a measured RSL $A[n, L]$ is given by [5]

$$\begin{aligned} A[n, L] &= A_p[n, L] + A_w[n] + A_v[n, L] \\ &\quad + A_0[L] + r[n] + q[n] \text{ dB} \\ n &= 1, \ldots, N. \end{aligned} \tag{1}$$

We take a set of $n = 1, \ldots, N$ samples per each ML, where:

1) $L$—link length;
2) $A_p[n, L]$—path-integrated precipitation attenuation;
3) $A_v[n, L]$—other-than-rain-induced attenuation, resulting primarily from the atmospheric water vapor [37];
4) $A_0[L]$—free-space propagation loss;
5) $A_w[n]$—wet/moist antenna attenuation;
6) $q[n]$—quantization noise;
7) $r[n]$—white noise.

We note that $A_w[n]$ is independent of the link length as opposed to $A_p[n, L]$ and $A_v[n, L]$ being dependent of path length and are considered here as channel interferences.

In cellular backhaul transmission systems, the RSL is typically quantized. For simplicity, we approximate the quantization effect using additive quantization noise $q[n]$. It is modeled as an additive uniformly distributed random process with variance $\frac{\Delta^2}{12}$, where $\Delta$ is the quantization interval. This approximation is valid for $A_p[n, L]$, $A_w[n]$ and $A_v[n, L]$ as long as their dispersion is higher than the quantization interval [5]. $r[n]$ is a measurement noise at the ML receiver, and is assumed to be an additive Gaussian noise. Since the latter is added at the ML receiver, it does not dependent on the link length.

In this study, we assume that no precipitation was present during the detection interval $N$, i.e., $A_p[n, L] = 0$. This assumption was validated using rainfall data taken from the Israeli Meteorological Service (IMS). However, we note that one can use the methods suggested in [38] or [8] for identifying dry periods (when no rain occurred). It is important to note that each link comprises a transmitter and receiver which are deployed at different spatial locations.

The idea of detecting moist antenna perturbations using ML lies on the principle that the attenuation is derived only due to the water film found on the microwave antenna itself and thus it can be determined whether attenuation drop observed simultaneously by multiple links, found in the same observed region, is independent of link length. We assume here homogeneity of the water vapor and dew in the observed field. Namely, all ML in the area examined are assumed to be affected by the same moist antenna-induced attenuation and by the same water vapor effect, while the latter is being proportional to the link length. The assumption, then, is that on days when dew existed, it simultaneously wet all of the microwave antennas in the observed region. In reality, it is possible, e.g., that only one of the two antennas that comprise the link was wet, but if attenuation was detected on the link, the assumption is that the wetting was simultaneous at both antennas. There has not

been much research investigating the spatial distribution of dew, however, recent work by Rowlandson [30] shows that over an area of 1 km$^2$, dew was observed simultaneously by different dew gauges located several hundreds of meters apart, and over separate dew events. In order to justify the assumption of the simultaneous occurrence of dew in this research, we adopted a conservative definition of a dew event. An event was considered dewy during times when all five meteorological stations measured RH of at least 90% and the LWS identified dew.

Under these assumptions, the attenuation model (1) of the $i$th ML from a set of $M$ links reduces to

$$A_i[n,L] = A_w[n] + L_i \cdot A_v[n] + A_{0i}[L] + r_i[n] + q_i[n] \text{ dB}$$
$$n = 1,\ldots,N,\ i = 1,\ldots,M. \quad (2)$$

Our goal is to decide whether moist antenna attenuation, ascribed to dew, is present or is it only the water vapor induced attenuation which is observed. Therefore, the attenuation model (2) can be transformed into a binary hypothesis test aimed for detecting the moist antenna losses

$$\mathcal{H}_0:\ A_i[n,L] = L_i \cdot A_v[n] + A_{0i}[L] + r_i[n] + q_i[n]$$
$$\mathcal{H}_1:\ A_i[n,L] = A_w[n] + L_i \cdot A_v[n] + A_{0i}[L] + r_i[n] + q_i[n]$$
$$n = 1,\ldots,N,\ i = 1,\ldots,M. \quad (3)$$

In typical conditions, water vapor is present in the atmosphere with different concentrations at different altitudes. Those concentrations vary with time and space; however, spatial variations are neglected here. $\mathcal{H}_0$ is, therefore, defined as the null hypothesis and is ascribed to the attenuation fluctuations induced by variations in the atmospheric humidity. $\mathcal{H}_1$ is defined as the moist antenna attenuation hypothesis.

Typically, dew is a phenomenon that is present for at least a few hours after emerging while the absolute humidity characteristically varies more slowly over time [33]. Therefore, under these assumptions, we consider their attenuations $A_w[n]$ and $A_v[n]$ as constant transient signals of unknown arrival times $n_w$ and $n_v$ and of unknown durations $\tau_w$ and $\tau_v$, respectively.

In our problem, we assume that the base-line attenuation of each link $i$ is caused by free-space propagation loss together with the absolute humidity attenuation that exists in the atmosphere. In dewy nights, the RH typically exceeds the threshold of 85% and therefore excess water-vapor-induced attenuation is expected. In Fig. 1, we exemplify the water vapor attenuation as a function of frequency [39] for a typical dry summer afternoon and dewy summer night in Israel [33]. The gray curve denotes the water vapor attenuation, in typical late afternoon conditions, where the RH is about 60% and the temperature is 25 °C. The black curve is the water vapor attenuation exemplifying early morning conditions where the RH is about 90% and the temperature is about 18 °C. The difference between the black and gray curves is denoted by the dashed curve signifying the additional water vapor induced attenuation $\Delta A_v[n]$, created due to the typical differences between the early morning humidity and that of the late afternoon. The typical water vapor attenuation during the late afternoon, together with the unknown zero level attenuation $A_{0i}[L]$ are defined as an unknown mean defined as the base-line attenuation for each link $\mu_i$.

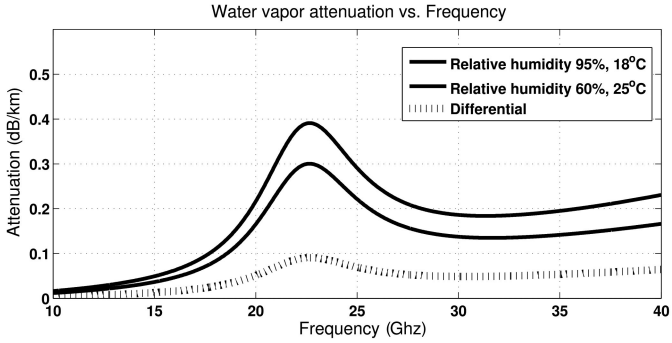


Fig. 1. Water vapor attenuation versus frequency in a typical dewy summer night in Israel. The gray curve is the water vapor attenuation, in the late afternoon, and the black curve is the water vapor attenuation, in early morning. The dashed curve is the differential water vapor attenuation. The meteorological data are based on [33] and on measurements from meteorological stations in the observed region.

In each link $i$, we model the noise measurement $r_i[n]$ and the quantization noise $q_i[n]$ by an additive white Gaussian noise (AWGN) $w_i[n]$ of unknown variance $\sigma^2$, meaning that we only use the second-order statistics of the real noise. This substitution leads to suboptimal parameter estimation, in the estimation step of the GLRT solution. In Section IV, we discuss and demonstrate the effects of this assumption on the detection performance. Additionally, we assume that the noise processes at the different sensors are independent and identically distributed (IID).

Notably, the binary hypothesis testing problem (3) is a specific problem of detecting an unknown deterministic transient signal $A_w[n]$ embedded within the interference signal. The difference between the two signals is that the moist antenna attenuation signal $A_w[n]$ affects all ML identically, while the interference signal (additional water vapor attenuation signal) affects each link proportionally to its length $L_i$.

Finally, the binary hypothesis testing problem is reduced to

$$\mathcal{H}_0:\ A_i[n,L] = L_i \cdot \Delta A_v[n\,;\,\tau_v\,,n_v] + \mu_i + w_i[n]$$
$$\mathcal{H}_1:\ A_i[n,L] = A_w[n\,;\,\tau_w\,,n_w]$$
$$+ L_i \cdot \Delta A_v[n\,;\,\tau_v\,,n_v] + \mu_i + w_i[n]$$
$$n = 1,\ldots,N,\ i = 1,\ldots,M. \quad (4)$$

Note that under each hypothesis $\mathcal{H}_0$ and $\mathcal{H}_1$, there are unknown parameters. Under $\mathcal{H}_0$, we define the $(M+4)$ dimensional vector of unknown parameters as $\underline{\theta}_0 \triangleq [\Delta A_v, n_v, \tau_v, \underline{\mu}^T, \sigma^2]^T$, whereas under $\mathcal{H}_1$, the $(M+7)$ dimensional vector of unknown parameters is defined as $\underline{\theta}_1 \triangleq [A_w, n_w, \tau_w, \Delta A_v, n_v, \tau_v, \underline{\mu}^T, \sigma^2]^T$. In (4), $A_w$ is the unknown constant moist antenna attenuation and $\Delta A_v$ is the unknown constant additional water vapor attenuation per unit of link length. The signal loss is a negative quantity and thus $A_w < 0$ and $\Delta A_v < 0$. One can note that $A_w, n_w$, and $\tau_w$ are the unknown parameters of the desired signal, while $\Delta A_v, n_v$, and $\tau_v$ are the unknown parameters of the interference signal. $\underline{\mu} \triangleq [\mu_1,\ldots,\mu_M]^T$ is $(M \times 1)$ vector consisting of the $M$ unknown measurement means (base-line attenuations).

### B. Method

In our detection problem, no prior information concerning the probabilities of the various hypotheses exists, and we can see that the pdf for each assumed hypothesis is not completely known. The uncertainty is expressed by including unknown non random parameters in the pdf. In such a case, when no uniformly most powerful (UMP) test [40] exists, the GLRT is commonly used to provide a solution [36]. The ln version of the GLRT for the binary hypothesis testing model (4) is of the form

$$L_G(\underline{X}) = \ln\left(\frac{P(\underline{X}\,;\,\hat{\underline{\theta}}_1,\,\mathcal{H}_1)}{P(\underline{X}\,;\,\hat{\underline{\theta}}_0,\,\mathcal{H}_0)}\right) \underset{\mathcal{H}_0}{\overset{\mathcal{H}_1}{\gtrless}} \gamma \tag{5}$$

where $P(\underline{X}\,;\,\underline{\theta}_1\,,\,\mathcal{H}_1)$ is the pdf of the received signal $\underline{X} \triangleq [A_1[1,L_1],\ldots,A_1[N,L_1],\ldots,A_M[1,L_M],\ldots,A_M[N,L_M]]^T$ under $\mathcal{H}_1$ with the unknown parameters vector $\underline{\theta}_1$, while $P(\underline{X}\,;\,\underline{\theta}_0\,,\,\mathcal{H}_0)$ is its pdf under $\mathcal{H}_0$ with the unknown parameters vector $\underline{\theta}_0$. $\hat{\underline{\theta}}_1$ is the maximum likelihood estimates (MLEs) [41] of $\underline{\theta}$ assuming $\mathcal{H}_1$ is true [maximizes $P(\underline{X}\,;\,\underline{\theta}_1\,,\,\mathcal{H}_1)$], and $\hat{\underline{\theta}}_0$ is the the MLE of $\underline{\theta}$ assuming $\mathcal{H}_0$ is true (maximizes $P(\underline{X}\,;\,\underline{\theta}_0\,,\,\mathcal{H}_0)$).

While there is no optimality associated with the GLRT, in some cases, it can be shown that the GLRT is asymptotically optimal, in the invariant sense [42], and in practice, it appears to acquire satisfying solutions. This test, in addition to signal detection, also provides information about the unknown parameters since the first step in computing (5) is to find the MLEs under each hypothesis.

Let us begin with evaluating the MLEs under each hypothesis. The MLE of $\underline{\theta}_0$ under $\mathcal{H}_0$ is found by maximizing the log likelihood function $L(\underline{X};\,\underline{\theta}_0)$

$$\begin{aligned}&\max_{\underline{\theta}_0}\{L(\underline{X}\,;\,\underline{\theta}_0)\}\\ &= \max_{\Delta A_v, n_v, \tau_v, \underline{\mu}, \sigma^2}\left\{-\frac{MN}{2}\ln\left(2\pi\sigma^2\right)\right.\\ &\left.-\sum_{i=1}^{M}\left(\frac{\|\underline{x}_i - L_i\cdot\Delta A_v\cdot h_v(n_v,\tau_v) - \mu_i\cdot\underline{1}\|^2}{2\sigma^2}\right)\right\}\end{aligned} \tag{6}$$

where $\underline{x}_i \triangleq [A_i[1,L_i],\ldots,A_i[N,L_i]]^T$, $\underline{1}_{N\times 1} \triangleq [1,\ldots,1]^T$, $h_v(n_v,\tau_v)$ is an $(N\times 1)$ vector, $h_{v\,n}\in\{0,1\}$, and $\|\underline{a}\|^2 \triangleq \underline{a}^T\cdot\underline{a}$.

*Theorem 1:* The MLEs of $\Delta A_v$ , $n_v$ , $\underline{\mu}$, and $\sigma^2$, which maximize (6), when the duration of the signal $\tau_v$ is fixed, and under the constraint that $\Delta\hat{A}_v \le 0$, are given by

1) $\hat{n}_v = \min_{n_v}\left\{\sum_{n=n_v}^{n_v+\tau_v-1} x_s[n]\right\}$, where $x_s[n] \triangleq \frac{1}{\left(\sum_{j=1}^{M} L_j^2\right)}$ $\sum_{i=1}^{M}(L_i\cdot x_i[n])$;
2) $\Delta\hat{A}_v = \frac{1}{\tau_v}\sum_{n=\hat{n}_v}^{\hat{n}_v+\tau_v-1} x_s[n] - \frac{1}{(N-\tau_v)}\sum_{n\notin[\hat{n}_v,\hat{n}_v+\tau_v-1]} x_s[n]$;
3) $\hat{\mu}_i = \frac{1}{N}\left(\sum_{n=1}^{N} x_i[n] - L_i\cdot\Delta\hat{A}_v\cdot\tau_v\right)$, $i=1,\ldots,M$;
4) $\hat{\sigma}^2 = \frac{1}{NM}\sum_{i=1}^{M}\|\left(\underline{x}_i - L_i\cdot\Delta\hat{A}_v\cdot h(\hat{n}_v,\tau_v) - \hat{\mu}_i\cdot\underline{1}\right)\|^2$.

*Proof:* The proof is given in Appendix A.

Bearing in mind the above, the MLE of $n_v$ under the constraint $\Delta\hat{A}_v \le 0$ from $M$ sensors is simply weighted summing their measurements, and looking for the initiating sample (time of arrival) where a time window of the sum with duration $\tau_v$ is minimal. The MLE of $\Delta A_v$, $\underline{\mu}$, and $\sigma^2$, when inserting the MLE of $n_v$, are found by the regular solution of a linear model Gaussian problem.

The MLE of $\tau_v$ is found by inserting $\Delta\hat{A}_v$ , $\hat{n}_v$ , $\hat{\underline{\mu}}$, and $\hat{\sigma}^2$ (Theorem 1) into (6), and searching for the value of $\tau_v \in [\tau_1,\tau_2]$ that achieves the maximum value, where $\tau_1$ and $\tau_2$ are *a priori* thresholds of the duration of the signal $\Delta A_v$, meaning that the minimum duration of the signal is $\tau_1$ and the maximum duration is $\tau_2$

$$\hat{\tau}_v = \min_{\tau_v\,\in\,[\tau_1,\tau_2]}\left\{\ln\left(2\pi\hat{\sigma}^2\right)\right\}. \tag{7}$$

Note that we assume in (7) that the observation interval $N$ is longer than the duration of the additional water vapor attenuation signal $N > \tau_2$, i.e., we choose observation interval that lasts longer than a typical water vapor phenomena (reasonable under typical Israeli weather conditions, as aforementioned [33]).

The MLE of $\theta_1$ under $\mathcal{H}_1$ is found by maximizing the log likelihood function $L(\underline{X}\,;\,\underline{\theta}_1)$

$$\begin{aligned}&\max_{\underline{\theta}_1}\{L(\underline{X}\,;\,\underline{\theta}_1)\}\\ &= \max_{\underline{\theta}_1}\left\{-\frac{MN}{2}\ln\left(2\pi\sigma^2\right) - \frac{1}{2\sigma^2}\sum_{i=1}^{M}(\|\underline{x}_i - A_w\cdot h_w(n_w,\tau_w)\right.\\ &\left.-L_i\cdot\Delta A_v\cdot h_v(n_v,\tau_v) - \mu_i\cdot\underline{1}\|^2)\right\}\end{aligned} \tag{8}$$

where $h_w(n_w,\tau_w)$, as $h_v(n_v,\tau_v)$, is an $(N\times 1)$ vector, $h_{w\,n}\in\{0,1\}$.

The appearance of dew is highly dependent on the atmospheric RH. The threshold RH above which dew is likely to emerge can be assumed to be 85% [33]. Due to this dependence we assume that moist antenna attenuation, which is caused by dew, can appear only during high RH conditions, i.e., during times when additional water-vapor-induced attenuation is expected to appear. This assumption is reasonable, since the ascension of humidity induces additional water vapor attenuation, and when it exceeds approximately the threshold of 85%, moist antenna attenuation is likely to emerge. Mathematically, that means that under $\mathcal{H}_1$ we assume that $n_w \ge n_v$ and $n_w + \tau_w < n_v + \tau_v$, i.e., the desired signal $A_w[n\,;\,n_w,\tau_w]$ appears only during the interference signal $\Delta A_v[n\,;n_v,\tau_v]$. We use this assumption to facilitate the MLE solution under $\mathcal{H}_1$ (8).

The MLE solution for $\theta_1$ is a 4-D search over $n_w$ , $\tau_w$ , $n_v$, and $\tau_v$, and for any combination of these four parameters, we deal with a quadratic optimization problem under constraints ($\hat{A}_w \le 0$ , $\Delta\hat{A}_v \le 0$). Note that the MLEs of $\Delta A_v, n_v, \tau_v, \underline{\mu}$, and $\sigma^2$ are different under each hypothesis.

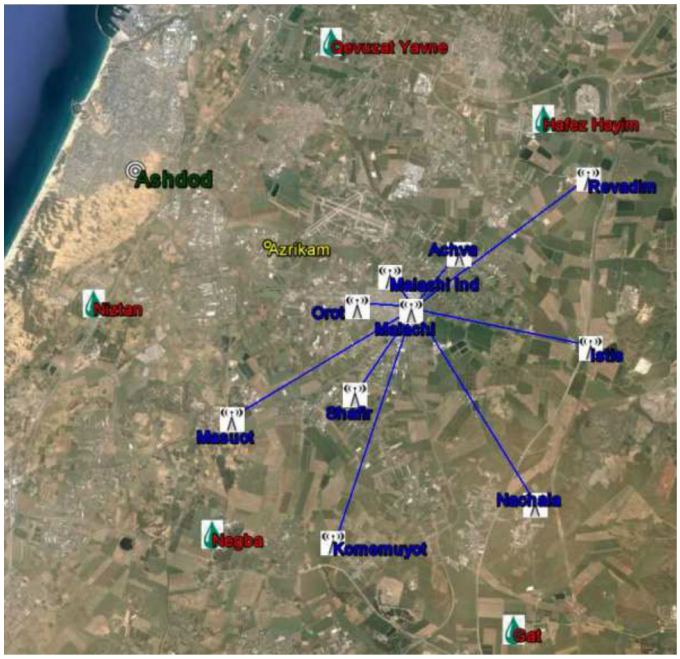


F2:1 Fig. 2. Map of MLs (lines), meteorological stations (drop signs), and LWS
F2:2 (circle sign).

363 Finally, we substitute the estimates, $\hat{\underline{\theta}}_1$ and $\hat{\underline{\theta}}_0$, into (5) in
364 order to get the GLRT test

$$L_G(\underline{X}) = -\frac{MN}{2}\ln\left(2\pi\hat{\sigma}_1^2\right) - \frac{MN}{2} + \frac{MN}{2}\ln\left(2\pi\hat{\sigma}_0^2\right) + \frac{MN}{2} = \frac{MN}{2}\ln\left(\frac{\hat{\sigma}_0^2}{\hat{\sigma}_1^2}\right) \underset{\mathcal{H}_0}{\overset{\mathcal{H}_1}{\gtrless}} \gamma \tag{9}$$

365 where $\hat{\sigma}_1^2$ is the estimation of $\sigma^2$ under $\mathcal{H}_1$ and $\hat{\sigma}_0^2$ is under $\mathcal{H}_0$.
366 The threshold $\gamma$ is set to determine the desired false alarm rate
367 using standard techniques [34]. In Section IV, we present the
368 experimental ROC obtained.

## 369 III. Experimental Setup and Model Assumptions

370 Commercial MLs operate at frequencies of tens of GHz, at
371 ground level altitudes. The RSL measurements are quantized
372 in steps of several decibels down to 0.1 dB, typically. Built-in
373 facilities enable RSL recording at various temporal resolutions,
374 depending on the type of the equipment (typically between once
375 per minute and once per day).
376 In this study, a microwave system comprised fixed terrestrial
377 line-of-sight links, employed for data transmission between cel-
378 lular base stations was used. We focused on 18 ML spread
379 across central Israel as described in Fig. 2. The technical spec-
380 ifications of the ML used are denoted in Table I. Each link
381 provides RSL records in 1 min intervals with a quantization
382 level of 1 dB. As can be seen in Table I, four different frequen-
383 cies were used, however, since the algorithm aims at detection
384 purposes only (i.e., not estimation of the different parame-
385 ters) the effect of frequency dependence on attenuation was
386 neglected. This action can be justified by the following reasons:
387 the algorithm estimates the excess water vapor attenuation.

TABLE I T1:1
Microwave Links T1:2

| ML name | Frequency (GHz) | Length (km) |
|---|---|---|
| K. Malachi—Orot | 18.82/17.81 | 1.9 |
| K. Malachi—Achva | 23.75/22.075 | 2.6 |
| K. Malachi—Revadim | 18.82/17.81 | 8 |
| K. Malachi—Nachala | 18.82/17.81 | 8 |
| K. Malachi—M. Izhak | 18.958/17.948 | 7.44 |
| K. Malachi—Komemiyot | 18.958/17.948 | 8.5 |
| K. Malachi—Istis | 18.82/17.81 | 6.5 |
| K. Malachi—K. Malachi Ind | 23.275/22.075 | 1.4 |
| K. Malachi—Shafir | 23.275/22.075 | 3.5 |

388 However, as depicted in Fig. 1, the differential water vapor
389 attenuation is weakly dependent on frequency. The algorithm
390 also calculates the attenuation due to antenna wetting which is
391 known to be weakly dependent on frequency, particularly at the
392 given relatively narrow frequency range [43]. In Section IV, we
393 verify this assumption.
394 In order to quantify and validate the results obtained using
395 the proposed technique, we used the LWS for detecting the
396 dewy events. The LWS is located in the vicinity of the
397 microwave system as illustrated in Fig. 2. In addition, RH
398 measurements from five meteorological stations, as shown in
399 Fig. 2 were utilized. The RH measurements in conjunction
400 with the LWS detections determined which of the events was
401 dewy. An event was considered dewy during times when all
402 five meteorological stations measured RH of at least 90% and
403 the LWS identified dew. Under these conditions, these mea-
404 surements were then compared to the microwave system wet
405 antenna detections acquired using the proposed methodology.
406 Notably, some disparities are expected between the different
407 ways of measuring a moist event (i.e., dew versus wet antenna)
408 as discussed in the conclusions. The justification for the com-
409 parison made between the two observations arises from the fact
410 that both phenomena, dew and moist antenna, appear when-
411 ever the condensation rate exceeds evaporation rate during
412 times of high atmospheric RH. As a consequence, the detec-
413 tion of moist antenna phenomenon can point to the presence of
414 dew, as will be exemplified in the next section. It is important
415 to note that moist antenna phenomenon cannot be considered
416 straightforwardly as dew, as will be discussed in the conclusion.

## 417 IV. Results

418 We applied the GLRT (9) to RSL measurements which were
419 taken from 40 nights (events) during the months of February
420 to July 2010. Based on measurements made with meteorologi-
421 cal instruments, 20 events were detected as dewy ones, and 20
422 were identified as dry, i.e., when no dew was observed by the
423 LWS (at RH $< 90\%$). The duration of each event (namely, the
424 observation interval $N$) was chosen to be 14 h ($N = 840$ sam-
425 ples), i.e., long enough to accommodate the variations within
426 the atmospheric phenomena observed (dew, water vapor) [33].
427 Under the no moist antenna hypothesis $\mathcal{H}_0$, we assume that the

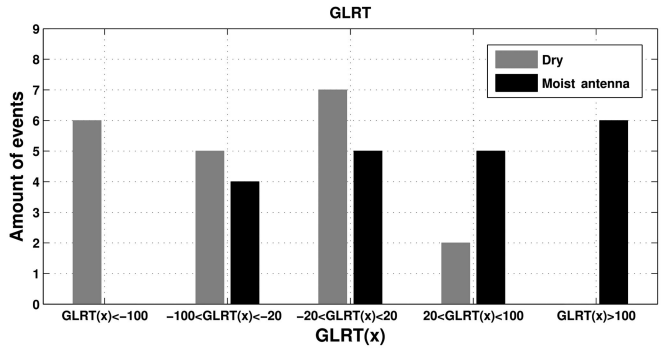


F3:1 Fig. 3. GLRT plane. Black bars are events that were considered as moist by
F3:2 the meteorological instruments, whereas the gray bars are events that were
F3:3 considered as just water vapor changes.

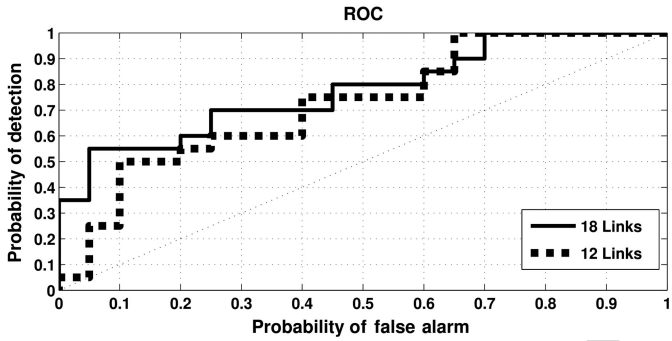


F4:1 Fig. 4. Probability of detection versus the probability of false alarm for the
F4:2 detection of moist antenna events, using the GLRT.

duration of the additional water vapor attenuation can receive any value for $\tau_v$ between 2 and 10 h, and under the moist antenna hypothesis $\mathcal{H}_1$, as explained in Section II, we add the assumption that $n_w \geq n_v$ and $n_w + \tau_w < n_v + \tau_v$.

The detection performance is presented by an ROC curve. The ROC illustrates the probability of detection $P_D$ (i.e., the algorithm indicated a moist antenna signal and in reality it was present) versus the probability of false alarm $P_{FA}$ (i.e., the algorithm indicated a moist antenna signal, but in reality it was not present).

Fig. 3 presents the GLRT's derived from measurements of 18 ML for the 40 events studied. The x-axis presents the GLRT plane, while the y-axis indicates the the number of events. The black bars are the events that were considered as moist by the RH measurements, from the five meteorological stations, and by the LWS identification. The gray bars are the events that were considered as just water vapor changes. It can be seen that there is a distinction between the two hypotheses, with moderate significance though. The ROC, in Fig. 4, was derived from the results depicted in Fig. 3. The figure presents the ROC of the GLRT based on measurements from 18 ML (black curve). For comparison, the ROC of the GLRT based on 12 ML (gray-dashed curve) is also given (the 12 ML were chosen to be the ones that operate at frequencies of around 17 and 18 GHz).

Table II details the estimation results of the GLRT for the additional water vapor attenuation and the moist antenna attenuation, based on five representative dewy events. As described previously in Section I, there is a relatively small amount of research dealing with monitoring other-than-precipitation

TABLE II T2:1
ESTIMATION RESULTS T2:2

| Date | $\Delta\hat{A}_v\left(\frac{\text{dB}}{\text{km}}\right)$ | $\hat{A}_w$ (dB) |
|---|---|---|
| 19.2.10–20.2.10 | $-0.028$ | $-0.37$ |
| 26.3.10–27.3.10 | $-0.069$ | $-0.67$ |
| 6.4.10–7.4.10 | $-0.029$ | $-0.52$ |
| 28.5.10–29.5.10 | $-0.04$ | $-0.15$ |
| 31.5.10–1.6.10 | $-0.027$ | $-0.74$ |

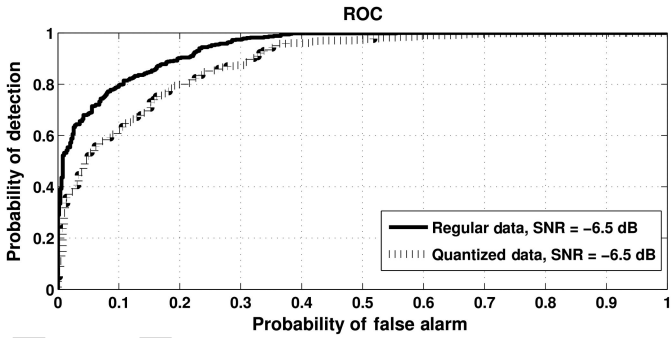


Fig. 5. Probability of detection versus the probability of false alarm for the F5:1
GLRT using quantized data and un-quantized data. In all the events, the true F5:2
signal was $A_w = 0.15$, the true interference signal was $A_v = 0.05$, and the F5:3
true variance of the Gaussian noise was $\sigma^2 = 0.1$. F5:4

phenomena using measurements from ML. As a consequence, currently, there is a limited capacity to compare and verify results in this area. However, it is notable that the moist antenna estimation results are of the same order of magnitude as those found by Hening and Stanton [17]. They found that the attenuation caused by dew at 20 GHz is approximately 0.5 dB. Moreover, the additional water vapor attenuation results obtained are of the same order comparing to the excessive water vapor curve depicted in Fig. 1, when focusing on the relevant frequencies.

The quantization noise is also a factor that may strongly affect the detection performance. Notably, the magnitude of the water vapor and moist antenna excess attenuation are of the same order as that of the quantization interval. Hence, the algorithm-based estimates are impaired. In order to examine this effect, a comparison between the GLRT ROCs derived for quantized and un-quantized data was produced by a computer simulation, as presented in Fig. 5. The GLRT (9) was applied on 1 dB quantized data and un-quantized data for 1000 events simulated (500—moist antenna events, 500—water vapor changes events) using 4 links ($M = 4$). The true values chosen of $A_w$ and $A_v$, are based on values found in literature.

## V. CONCLUSION

The results point to the potential of detecting dewy episodes using already existing commercial ML. The results (Figs. 3 and 4) demonstrate that adding links improves performance of the detection algorithm. The 18 ML-based curve (black) where frequencies of 17–23 GHz were used achieved better results than the 12 ML-based curve (gray) where frequencies of only

17–18 GHz were used. In this case, the amount of links had a greater impact on the detection performance than the accuracy of the model. Therefore, it is reasonable to assume that the attenuation due to excessive water vapor and moist antenna on the ML is weakly dependent on frequency.

Figs. 3 and 4 present a moderate distinction between the two hypotheses. While further investigation is required concerning this issue, we can point to the following aspects that would affect these results: first, as mentioned, moist antenna phenomena cannot straightforwardly be considered as dew. Therefore, since we validate the performance of the GLRT algorithm by the LWS, which identifies dew, there is a possibility that even though the sensor identified the event as dewy, a moist layer did not accumulate on the antenna surface in a specific event. Having said that, it is possible then that the four negative events (black bar) observed in Fig. 3 are an example of such cases. That is, these events were detected as dewy by the LWS while the GLRT algorithm classified them as no moist antenna events.

Fig. 5 points to a significant gap between the ROC curve of quantized data and that of un-quantized data, for SNR $=$ $-6.5$ dB $\left(\text{SNR} \triangleq 10\log\left(\frac{A_w^2}{\sigma^2}\right)\right)$. However, it should be noted that more sensitive microwave systems exists with digital quantization of, e.g., 0.1 dB [11], [14]. Hence, it is expected that applying the algorithm on such RSL data will improve accuracy when compared to microwave systems with coarser sensitivity (as the system utilized in this study).

While a principle feasibility has been demonstrated, additional experimental and modeling research are required. The contribution of transmission loss due to atmospheric phenomena (e.g., fog) and due to the wettings of the antennas, as well as the effect of antenna elevation (ranging from several meters to several tens of meters) off the surface should be studied. Further experimental verification should also take into account the inherent uncertainty of reference data, including technical limitations of dew meters, difference in wetting properties of materials, in particular: the microwave radomes are artificial materials with different thermal properties comparing to those of soil or vegetation pallets. Moreover, the difference of orientation of the wetting surfaces, microwave radomes are vertical surfaces while typical dew meters are horizontal surfaces.

Since dew has a cardinal part in various ecological processes, the numerous microwave antennas, acting as a dew detector unit, have the potential to shed light on the role of this phenomenon in the local and global ecosystems.

## Appendix A
## Proof of Theorem 1

Let us consider first the case of $M = 1$. Thus, when using one sensor and when the duration of the signal $\tau_v$ is fixed, (6) reduces to

$$\max_{\Delta A_v, n_v, \mu, \sigma^2} \left\{ -\frac{N}{2}\ln\left(2\pi\sigma^2\right) - \left( \frac{\|\underline{x} - L\cdot\Delta A_v \cdot h_v(n_v,\tau_v) - \mu\cdot\underline{1}\|^2}{2\sigma^2} \right) \right\} \tag{A1}$$

The MLE of $\sigma^2$, when $\Delta A_v$ , $n_v$, and $\mu$ are fixed, is given by

$$\hat{\sigma}^2 = \frac{1}{N}\left(\|\underline{x} - L\cdot\Delta A_v\cdot h_v(n_v,\tau_v) - \mu\cdot\underline{1}\|^2\right) \tag{A2}$$

substituting (A2) into (A1) yields

$$\min_{\Delta A_v, n_v, \mu} \left\{ \left(\|\underline{x} - L\cdot\Delta A_v\cdot h_v(n_v,\tau_v) - \mu\cdot\underline{1}\|^2\right)\right\}. \tag{A3}$$

The MLE of $\mu$, when $A_v$ and $n_v$ are fixed, is given by

$$\begin{aligned}\hat{\mu} &= \left(\underline{1}^T\cdot\underline{1}\right)^{-1}\cdot\underline{1}^T\cdot\left(\underline{x} - L\cdot\Delta A_v\cdot h_v(n_v,\tau_v)\right) \\ &= \frac{1}{N}\left(\sum_{n=1}^{N} x[n] - L\cdot\tau_v\cdot\Delta A_v\right)\end{aligned} \tag{A4}$$

substituting (A4) into (A3) and simplifying yields

$$\begin{aligned}\min_{\Delta A_v, n_v} \big\{ &\underline{x}^T\cdot Q\cdot\underline{x} - 2\cdot L\cdot\Delta A_v\cdot\underline{x}^T\cdot Q\cdot h_v(n_v,\tau_v) \\ &+ L^2\cdot(\Delta A_v)^2\cdot h_v(n_v,\tau_v)^T\cdot Q\cdot h_v(n_v,\tau_v)\big\}\end{aligned} \tag{A5}$$

where $Q \triangleq \left(I_{N\times N} - \frac{1}{N}\cdot\underline{1}\cdot\underline{1}^T\right)$ is a projection matrix.

Note that the expression $\underline{x}^T\cdot Q\cdot\underline{x}$ in (A5) is independent of $A_v$ or $n_v$ and therefore (A5) reduces to

$$\begin{aligned}\min_{\Delta A_v, n_v} \big\{ &-2\cdot\Delta A_v\cdot(\underline{x}^T/L)\cdot Q\cdot h_v(n_v,\tau_v) \\ &+ (\Delta A_v)^2\cdot h_v(n_v,\tau_v)^T\cdot Q\cdot h_v(n_v,\tau_v)\big\}\end{aligned} \tag{A6}$$

The MLE of $\Delta A_v$, when $n_v$ is fixed, is given by

$$\begin{aligned}\Delta\hat{A}_v &= \frac{1}{L}\left(h_v(n_v,\tau_v)^T Q h_v(n_v,\tau_v)\right)^{-1}\cdot h_v(n_v,\tau_v)^T Q\underline{x} \\ &= \frac{1}{L}\left(\frac{1}{\tau_v}\sum_{n=n_v}^{n_v+\tau_v-1} x[n] - \frac{1}{(N-\tau_v)}\sum_{n\notin[n_v,n_v+\tau_v-1]} x[n]\right)\end{aligned} \tag{A7}$$

Note that

$$h_v(n_v,\tau_v)^T\cdot Q\cdot h_v(n_v,\tau_v) = \tau_v - \frac{\tau_v^2}{N} \tag{A8}$$

using (A8) and rearranging (A7) yields

$$\Delta\hat{A}_v\cdot\left(\tau_v - \frac{\tau_v^2}{N}\right) = \left(\underline{x}^T/L\right)\cdot Q\cdot h_v(n_v,\tau_v) \tag{A9}$$

substituting (A8) and (A9) into (A6) yields

$$\max_{n_v}\left\{\left(\tau_v - \frac{\tau_v^2}{N}\right)\cdot\left(L\cdot\Delta\hat{A}_v\right)^2\right\} \tag{A10}$$

We use the prior information under $\mathcal{H}_0$; hence, the expression $\left(\tau_v - \frac{\tau_v^2}{N}\right)$ is positive $\forall\,\tau_v \in [\tau_1,\tau_2]$, where $\tau_2 < N$, so (A10) becomes

$$\max_{n_v}\left\{\left(L\cdot\Delta\hat{A}_v\right)^2\right\} = \max_{n_v}\left\{\left(\frac{1}{\tau_v}\sum_{n=n_v}^{n_v+\tau_v-1} x[n] - \frac{1}{(N-\tau_v)}\sum_{n\notin[n_v,n_v+\tau_v-1]} x[n]\right)^2\right\} \tag{A11}$$

Using the fact that $\Delta\hat{A}_v \leq 0$, (A11) reduces to

$$\min_{n_v}\left\{\frac{1}{\tau_v}\sum_{n=n_v}^{n_v+\tau_v-1}x[n]-\frac{1}{(N-\tau_v)}\sum_{n\notin[n_v,n_v+\tau_v-1]}x[n]\right\}$$

and therefore the MLE of $n_v$ is given by

$$\hat{n}_v=\min_{n_v}\left\{\sum_{n=n_v}^{n_v+\tau_v-1}x[n]\right\}. \tag{A12}$$

For the MLE of $\Delta A_v$, we insert $\hat{n}_v$ (A12) into (A7) and for the MLE of $\mu$, we insert $\hat{n}_v$ (A12) and $\Delta\hat{A}_v$ (A7) into (A4). The same process happens with the MLE of $\sigma^2$, where we insert $\hat{n}_v$, $\Delta\hat{A}_v$ and $\hat{\mu}$ into (A2).

Finally, we show how the case of $M>1$ is reduced to the case of $M=1$, when the measurements vector is $x_s[n]$. First, we find the MLE of $\sigma^2$ and for each sensor $i$ the MLE of $\mu_i$, when $\Delta A_v$ and $n_v$ are fixed, as in (A2) and (A4)

$$\hat{\sigma}^2=\frac{1}{NM}\sum_{i=1}^{M}\|\left(\underline{x}_i-L_i\cdot\Delta A_v\cdot h_v(n_v,\tau_v)-\mu_i\cdot\underline{1}\right)\|^2 \tag{A13}$$

$$\hat{\mu}_i=\frac{1}{N}\left(\sum_{n=1}^{N}x_i[n]-L_i\cdot\tau_v\cdot\Delta A_v\right),\ i=1,\ldots,M. \tag{A14}$$

Substituting (A13) and (A14) into (6) yields

$$\begin{aligned}&\min_{\Delta A_v,n_v}\left\{\sum_{i=1}^{M}\left(\|Q\underline{x}_i-L_i\cdot\Delta A_v\cdot Qh_v(n_v,\tau_v)\|^2\right)\right\}\\&=\min_{\Delta A_v,n_v}\left\{-2\cdot\Delta A_v\sum_{i=1}^{M}\left(L_i\cdot\underline{x}_i^T\right)Qh_v(n_v,\tau_v)\right.\\&\left.+\sum_{i=1}^{M}L_i^2\cdot(\Delta A_v)^2\cdot h_v(n_v,\tau_v)^TQh_v(n_v,\tau_v)\right\}\\&=\min_{\Delta A_v,n_v}\left\{-2\cdot\Delta A_v\frac{\sum_{i=1}^{M}\left(L_i\underline{x}_i^T\right)}{\sum_{j=1}^{M}L_j^2}Qh_v(n_v,\tau_v)\right.\\&\left.+(\Delta A_v)^2h_v(n_v,\tau_v)^TQh_v(n_v,\tau_v)\right\}\end{aligned} \tag{A15}$$

We can see that (A15) is the same optimization problem as (A6), except for the replacement of $\underline{x}^T$ by $\sum_{i=1}^{M}\left(L_i\cdot\underline{x}_i^T\right)$ and $L$ by $\sum_{j=1}^{M}L_i^2$, i.e., we replaced $\frac{\underline{x}^T}{L}$ by $\underline{x}_s^T$. Hence, the MLE of $\underline{\theta}_0$, which maximizes (6), is found by Theorem 1.

## ACKNOWLEDGMENT

This paper is dedicated to the newborn $Tal$, which means "dew" in Hebrew, the son of Debbie and weather expert Asaf Rayitsfeld from the IMS to whom we owe gratitude for the practical meteorological consultation. The authors are grateful to N. Dvela (Pelephone), Y. Dagan, Y. Eisenberg, E. Levi, S. Shilyan, and I. Alexandrovitz (Cellcom), H. B. Shabat, A. Shor, H. Mushvilli, and Y. Bar Asher (Orange) for providing the microwave data for our research. They also deeply thank the IMS for providing meteorological reference data. They extend special thanks to TAU research team members, for many fruitful discussion and valuable remarks: late Dr. R. Samuels, E. Heiman, Y. Liberman, O. Auslender, Y. Ostrometzky, R. Radian, and Y. Cantor.

## REFERENCES

[1] H. Messer, A. Zinevich, and P. Alpert, "Environmental monitoring by wireless communication networks," *Science*, vol. 312, no. 5774, p. 713, May 2006.

[2] H. Leijnse, R. Uijlenhoet, and J. N. M. Stricker, "Rainfall measurement using radio links from cellular communication networks," *Water Resour. Res.*, vol. 43, p. W03201, Mar. 2007.

[3] A. Zinevich, H. Messer, and P. Alpert, "Estimation of rainfall fields using commercial microwave communication networks of variable density," *Adv. Water Resour.*, vol. 31, pp. 1470–1480, Nov. 2008.

[4] A. Zinevich, H. Messer, and P. Alpert, "Frontal rainfall observation by a commercial microwave communication network," *Amer. Meteorol. Soc.*, vol. 48, pp. 1317–1334, Jul. 2009.

[5] A. Zinevich, H. Messer, and P. Alpert, "Prediction of rainfall intensity measurement errors using commercial microwave communication links," *Atmos. Meas. Techn.*, vol. 5, no. 3, pp. 1385–1402, 2010.

[6] Z. Wang, M. Schleiss, J. Jaffrain, A. Berne, and J. Rieckermann, "Using Markov switching models to infer dry and rainy periods from telecommunication microwave link signals," *Atmos. Meas. Techn.*, vol. 5, pp. 1847–1859, 2012.

[7] A. Gmeiner *et al.*, "Precipitation observation using microwave backhaul links in the alpine and pre-alpine region of southern Germany," *Hydrol. Earth Syst. Sci.*, vol. 16, no. 8, pp. 2647–2661, Aug. 2012.

[8] O. Harel and H. Messer, "Extension of the MFLRT to detect an unknown deterministic signal using multiple sensors, applied for precipitation detection," *IEEE Signal Process. Lett.*, vol. 20, no. 10, pp. 945–948, Oct. 2013.

[9] N. David, P. Alpert, and H. Messer, "The potential of cellular network infrastructures for sudden rainfall monitoring in dry climate regions," *Atmos. Res.*, vol. 131, pp. 13–21, Jan. 2013.

[10] H. Leijnse, R. Uijlenhoet, and J. N. M. Stricker, "Hydrometeorological application of microwave link: 1. Evaporation," *Water Resour. Res.*, vol. 43, p. W04416, Apr. 2007.

[11] N. David, P. Alpert, and H. Messer, "Novel method for water vapour monitoring using wireless communication networks measurements," *Atmos. Chem. Phys.*, vol. 7, pp. 2413–2418, Apr. 2009.

[12] N. David, P. Alpert, and H. Messer, Humidity Measurements Using Commercial Microwave Links, Aadvanced Trends in Wireless Communications. Croatia, Europe: InTech Publications, 2011.

[13] C. Chwala, H. Kunstmann, S. Hipp, and U. Siart, "A monostatic microwave transmission experiment for line integrated precipitation and humidity remote sensing," *Atmos. Res.*, vol. 144, pp. 57–62, Jul. 2013.

[14] N. David, P. Alpert, and H. Messer, "The potential of commercial microwave networks to monitor dense fog-feasibility study," *J. Geophys. Res. Atmos.*, vol. 180, no. 20, pp. 11750–11761, 2013.

[15] N. David, O. Sendik, H. Messer, and P. Alpert, "Cellular network infrastructure-the future of fog monitoring?," *Bull. Amer. Meteorol. Soc.*, vol. 96, no. 11, 2014, doi: 10.1175/BAMS-D-13-00292.1, in press.

[16] M. Schleiss, J. Rieckermann, and A. Berne, "Quantification and modeling of wet-antenna attenuation for commercial microwave links," *IEEE Geosci. Remote Sens. Lett.*, vol. 10, no. 5, pp. 1195–1199, Feb. 2013.

[17] R. E. Henning and J. R. Stanton, "Effects of dew on millimeter-wave propagation," *in Proc. IEEE Southeastcon Bringing Together Educ. Sci. Technol.*, Apr. 1996, pp. 684–687.

[18] AMS, *AMS Glossary of Meteorology*, 2nd ed. Boston, MA, USA: American Meteorological Society, 2000 [Online]. Available: http://amsglossary.allenpress.com/glossary/browse.

[19] A. A. Degen, A. Leeper, and M. Shachak, "The effect of slope direction and population density on water influx in a desert snail, Trochoidea seetzenii," *Funct. Ecol.*, vol. 6, pp. 160–166, 1992.

[20] M. Moffett, "An Indian ant's novel method for obtaining water," *Nat. Geogr. Res.*, vol. 1, no. 1, pp. 146–149, 1985.

[21] A. Danin, Y. Bar-Or, I. Dor, and T. Yisraeli, "The role of cyanobacteria in stabilization of sand dunes in southern Israel," *Ecol. Mediterr.*, vol. 15, pp. 55–64, 1989.

[22] O. Lange, G. Kidron, B. Budel, A. Meyer, E. Kilian, and A. Abeliovich, "Taxonomic composition and photosynthetic characteristics of the biological soil crusts covering sand dunes in the western Negev desert," *Funct. Ecol.*, vol. 6, no. 5, pp. 519–527, 1992.
[23] P. Petropoulosa, I. Gareth, P. K. Srivastavabc, and P. Ioannou-Katidisa, "An appraisal of the accuracy of operational soil moisture estimates from SMOS MIRAS using validated in situ observations acquired in a mediterranean environment," *Int. J. Remote Sens.*, vol. 35, pp. 5239–5250, Jul. 2014.
[24] Y. H. Kerr *et al.*, "The SMOS soil moisture retrieval algorithm," *IEEE Trans. Geosci. Remote Sens.*, vol. 50, no. 5, pp. 1384–1403, May 2012.
[25] A. M. Richard, D. Jeu, R. H. H. Thomas, and M. Owe, "Determination of the effect of dew on passive microwave observations from space," *Proc. SPIE Remote Sens. Agric. Ecosyst. Hydrol.*, Oct. 2005, vol. 5976, p. 597608.
[26] B. Hornbuckle, A. England, M. Anderson, and B. Viner, "The effect of free water in a maize canopy on microwave emission at 1.4 GHz." *Agric. For. Meteorol.*, vol. 138, pp. 180–191, Aug. 2006.
[27] B. Hornbuckle, A. England, and M. Anderson, "The effect of intercepted precipitation on the microwave emission of maize at 1.4 GHz," *IEEE Trans. Geosci. Remote Sens.*, vol. 45, no. 7, pp. 1988–1995, Jul. 2007.
[28] J. Du *et al.*, "Effect of dew on aircraft-based passive microwave observations over an agricultural domain," *J. Appl. Remote Sens.*, vol. 6, no. 1, pp. 063571-1–063571-10, Aug. 2012.
[29] P. C. Sentelhasa, A. D. Martab, S. Orlandinib, E. A. Santosc, T. J. Gillespiec, and M. L. Gleasond, "Suitability of relative humidity as an estimator of leaf wetness duration," *Agric. For. Meteorol.*, vol. 148, pp. 392–400, Mar. 2008.
[30] T. L. Rowlandson, "Leaf wetness: Implications for agriculture and remote sensing," Graduate Theses and Dissertations, Iowa State University, *Ames, IA, USA*, 2011.
[31] J. Ben-Asher, P. Alpert, and A. Ben-Zvi, "Dew is a major factor affecting the vegetation water use efficiency rather than a source of water in the eastern mediterranean," *Water Resour. Res.*, vol. 46, p. W10 532, 2010, doi: 10.1029/2008WR007484.
[32] M. Moro, A. Were, L. Villagarcia, Y. Canton, and F. Domingo, "Dew measurement by Eddy covariance and wetness sensor in a semiarid ecosystem of SE Spain," *J. Hydrol.*, vol. 335, pp. 295–302, Mar. 2007.
[33] Y. Golderich, *The Climate of Israel: Observation, Research and Application*. Ramat Gan, Israel: Bar-Ilan Press, 1998.
[34] S. Kay, Fundamentals of Statistical Signal Processing: Detection Theory. Englewood Cliffs, NJ, USA: Prentice-Hall, 1998.
[35] A. Overeem, H. Leijnse, and U. R, "Country-wide rainfall maps from cellular communication networks," *Proc. Nat. Acad. Sci.*, vol. 110, no. 8, pp. 2741–2745, 2013.
[36] H. Messer and M. Frisch, "Transient signal detection using prior information in the likelihood ratio test," *IEEE Trans. Signal Process.*, vol. 41, no. 6, pp. 2177–2192, Jun. 1993.
[37] D. Thomas and J. L. Frey, "The effects of the atmosphere and weather on the performance of a mm-wave communication link," *Appl. Microw. Wireless*, vol. 13, no. 1, pp. 76–80, Feb. 1997.
[38] M. Schleiss and A. Berne, "Identification of dry and rainy periods using telecommunciation microwave links," *IEEE Geosci. Remote Sens. Soc.*, vol. 7, no. 3, pp. 611–615, Jul. 2010.
[39] International Telecommunication Union (ITU), "Attenuation by atmospheric gases," ITU-Recommendations, R.I.-R. P. 676–6, 2005.
[40] L. L. Scharf, *Statistical Signal Processing*. Reading, MA, USA: Addison-Wesley, 1991.
[41] S. Kay, Fundamentals of Statistical Signal Processing: Estimation Theory. Englewood Cliffs, NJ, USA: Prentice-Hall, 1998.
[42] L. L. Scharf and B. Friedlander, "Matched subspace detectors," *IEEE Trans. Signal Process.*, vol. 42, no. 8, pp. 2146–2157, Aug. 2002.
[43] H. Leijnse, "Hydrometeorological appliction of microwave links," Ph.D. dissertation, Wageningen University, Wageningen, The Netherlands, 2007.

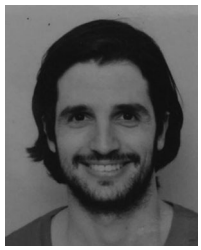

**Oz Harel** received the B.Sc. and M.Sc. (through the direct master's program) degrees in electrical engineering from the Faculty of Engineering, Tel Aviv University (TAU), Tel Aviv, Israel.

Currently, he works as Algorithm Engineer in the microwave communication industry. His research interests include statistical signal processing, remote sensing, and environmental monitoring.

**Noam David** received the B.Sc. (with distinction) and Ph.D. (through the direct doctoral track) degrees in geosciences from Tel Aviv University, Tel Aviv, Israel.

He currently holds a Postdoctoral position with the School of Civil and Environmental Engineering, Cornell University, Ithaca, NY, USA. His research interests include weather and atmospheric sciences, wave matter interaction, remote sensing, air quality, and environmental monitoring.

**Pinhas Alpert** received the Ph.D. degree in meteorology from the Hebrew University of Jerusalem, Jerusalem, Israel, in 1980.

He joined the Department of Geosciences, Tel Aviv University, Tel Aviv, Israel, in 1982, after a Postdoctorate at Harvard University, Cambridge, MA, USA. He is currently the Mikhael M. Nebenzahl and Amalia Grossberg Chair Professor of Geodynamics. He served as the Head of the Porter School of Environmental Studies, Tel-Aviv University, during 2008–2013, following 3 years as Head of the Department of Geosciences at Tel Aviv University. He established and Heads the Israel Space Agency Middle East Interactive Data Archive (ISA-MEIDA), Tel Aviv, Israel. He is a Co-Director of the GLOWA-Jordan River BMBF/MOS project to study the water vulnerability in the E. Mediterranean and served as the Israel Representative to the IPCC TAR WG1. His research interests include atmospheric dynamics, climate, numerical methods, limited area modeling, aerosol dynamics, and climate change.

**Hagit Messer** (F'00) received the Ph.D. degree in electrical engineering from Tel Aviv University (TAU), Tel Aviv, Israel.

After a Postdoctoral Fellowship with Yale University, New Haven, CT, USA, she joined the Faculty of Engineering, Tel Aviv University, in 1986, where she is a Professor of Electrical Engineering. During 2000–2003, she was on leave from TAU, serving as the Chief Scientist at the Ministry of Science. After returning to TAU, she was the Head of the Porter School of Environmental Studies (2004–2006) and the Vice President for Research and Development (2006–2008). Then, she has been the President of the Open University, and from October 2013, she serves as the Vice Chair of the Council of Higher Education, Jerusalem, Israel. She is an Expert in statistical signal processing with applications to source localization, communication and environmental monitoring. She has authored numerous journal and conference papers, and has supervised tens of graduate students.

Prof. Messer has been a member of Technical Committees of the Signal Processing Society since 1993 and on the Editorial Boards of the IEEE TRANSACTIONS ON SIGNAL PROCESSING, the IEEE SIGNAL PROCESSING LETTERS, the IEEE JOURNAL OF SELECTED TOPICS IN SIGNAL PROCESSING (J-STSP), and on the Overview Editorial Board of the Signal Processing Society journals.

# The Potential of Microwave Communication Networks to Detect Dew—Experimental Study

Oz Harel, Noam David, Pinhas Alpert, and Hagit Messer, *Fellow, IEEE*

***Abstract*—At microwave frequencies of tens of GHz, various hydrometeors cause attenuations to the electromagnetic signals. Here, we focus on the effect of liquid water films accumulating on the outer coverage of the microwave units during times of high relative humidity (RH). We propose a novel technique to detect moist antenna losses using standard received signal level (RSL) measurements acquired simultaneously by multiple commercial microwave links (MLs). We use the generalized likelihood ratio test (GLRT) for detecting a transient signal of unknown arrival time and duration. The detection procedure is applied on real RSL measurements taken from an already existing microwave network. It is shown that moist antenna episodes can be detected, information which provides the potential to identify dew, an important hydro-ecological parameter.**

***Index Terms*—Attenuation, commercial microwave links (MLs), dew, generalized likelihood ratio test (GLRT), received signal level (RSL).**

## I. Introduction

YEARS of research have developed the capacity for modeling, understanding and mitigation of atmosphere-induced reductions of the quality of wireless communication links. After exposing the idea of using measurements from commercial cellular operators for rainfall monitoring [1], [2], this field of research has been extensively studied and developed [3]–[9]. Notably, nearly all of the research in this field has focused on rainfall monitoring.

However, rain is not the only source for impairments to the received radio signals. In the presence of a clear line of sight, such propagation phenomena—diffraction, refraction, absorption, and scattering—may cause acute reductions. At frequencies above 10 GHz, some of them (absorption and scattering) are directly related to other atmospheric phenomena. Thus, it has also been shown that microwave links (MLs) have the potential to monitor phenomena aside from rain, such as areal evaporation [10], water vapor density [11]–[13], and even fog [14], [15].

Excess attenuation due to antenna wetting during rainfall episodes has been studied [5], [10], [16]. However, until now, this effect has been considered as a negative perturbation, causing additional attenuations to the radio signals and thus interfering with the ability to conduct accurate rain rate measurements. However, in some cases, this perturbation contains vital information, particularly during times of dew: whenever condensation rate exceeds evaporation rate, a thin layer of water droplets accumulates directly on the antenna surface or the external radome, causing moistening of the radio units. This water film may lead to a signal loss, which can be measured by the microwave system. This effect has been recently shown to cause additional losses to the microwave signals during heavy fog events [14]. At an earlier stage, Hening and Stanton [17] measured experimentally the microwave attenuation caused by dew using a parabolic reflector antenna. The experiment was conducted when a dew layer was known to be present on the antenna reflector. Then, the water layer was wiped off the antenna at a certain known time. As a result, the signal level at 20 and 27 GHz channels gained 0.5 and 1.5 dB, respectively, immediately after the dew layer was removed.

According to the American Meteorological Society (AMS), dew is defined as water condensed onto grass and other objects at ground level while the temperature of which have fallen below the dew-point of the surface air due to radiational cooling during night time [18].

The motivation for monitoring this phenomenon rises from various ecological aspects. Dew can serve as an important source of moisture for animals [19], [20] and biological crusts that can contribute to the stabilization of sand dunes [21], [22]. Terrestrial microwave radiation is sensitive to soil moisture, which is an important element of the hydrological cycle, and affects weather and climate [23]. By observing terrestrial microwave emission, satellites can map soil moisture variability spatially and temporally [24]. However, terrestrial microwave emission is also affected by water in vegetation as dew (or intercepted precipitation). As a result, bias caused by the presence of free water can introduce error to the soil moisture measurement [25]–[28]. Therefore, high spatio-temporal information about dew, if obtained, can potentially be used in combination with remote sensing satellites to improve the ability to derive more accurate observations of soil moisture [28].

The perspective regarding the dew-plants interaction is controversial: plant pathologists emphasize the negative role played by dew in the promotion of plant diseases [29]. This being the case, agricultural warning systems of plant diseases, that assist growers in deciding on the appropriate time to use preventative measures, use information concerning the duration of leaf wetness as an input [30]. On the other hand, it has been found recently that dew formation serves as an integral part in the

Manuscript received December 26, 2014; revised July 02, 2015; accepted July 25, 2015.

O. Harel and H. Messer are with the School of Electrical Engineering, Tel Aviv University, Tel Aviv, Israel (e-mail: ozharel@gmail.com; messer@eng.tau.ac.il).

N. David is with the School of Civil and Environmental Engineering, Cornell University, Ithaca, NY USA (e-mail: nd363@cornell.edu).

P. Alpert is with the Department of Geosciences, Tel Aviv University, Tel Aviv, Israel (e-mail: pinhas@post.tau.ac.il).

Color versions of one or more of the figures in this paper are available online at http://ieeexplore.ieee.org.

Digital Object Identifier 10.1109/JSTARS.2015.2465909

general strategy of vegetation water economy in the arid and semiarid zones [31]. However, the information regarding dew in the literature is scarce, in part due to the difficulty associated with its measurement [32], [33]. Thus, standard meteorological stations do not measure this parameter, and other facilities have limited applications.

Typical dew detection and measuring instruments include drosometers and the leaf wetness sensors (LWSs). The drosometer is a large surface comprised of fine fiber (wool, cotton) or metal plate. It measures the amount of accumulating dew per unit area per time. The measurements are made in the early morning, before the rising sun evaporates the dew. However, these observations are considered inaccurate, primarily since the slightest change in the surface that receives the moisture alters the quantity of dew that is caught. The LWS is an apparatus used for identifying leaf wetness (i.e., dew). The operating principle of this device is based on a simple electronic circuit, which is completed when water bridges two inter digitated electrodes. It measures the fraction of time that moisture accumulates and completes the electronic circuit.

The goal of this paper is to address the problem of identifying antenna wetting periods during dew episodes utilizing received signal level (RSL) measurements from a spatially distributed MLs network. A novel method to detect moist antenna attenuation periods is suggested based on *signal detection theory* [34]. The extremely high density of ML [1], [35], which can reach several tens of links deployed over a single square km, especially in urban areas [14], guarantees markedly higher coverage when compared to any other sensor system, or the spatial coverage achieved by dew gauges deployed in conventional ground stations.

Let us briefly specify the different signal processing stages. First, we extract the physical characteristics of the meteorological phenomena observed. Accordingly, the meteorological phenomena induced attenuation can be formulated as an unknown deterministic signal and respectively the classical binary hypothesis testing problem (signal detection problem) is defined, where we aim to detect an unknown deterministic signal embedded in the interference signal. Second, we use the generalized likelihood ratio test (GLRT) [36] in order to discriminate the moist antenna attenuation from other atmospheric impairments. Finally, we apply the suggested method on real RSL measurements taken from an already existing microwave network.

The performance of the proposed method is quantified by an experimental receiver operating characteristics (ROC) curve where the validation process is conducted using LWS and relative humidity (RH) data taken from standard meteorological stations.

## II. Model and Method

### A. Model

Environmental monitoring techniques, like other signal processing systems such as Radar and Communication, share the basic goal of being able to detect whether an event of interest occurred (e.g., rainfall and fog) and then extract information concerning the event. The former task, of decision-making, is usually termed *detection theory*. The degree of difficulty of these problems is directly related to the information concerning the signal and noise characteristics which can be modeled in terms of their probability density functions (pdfs). Accordingly, let us define the detection model and the effects of humidity and dew on a ML as unknown deterministic attenuation signals.

A simplified model for a measured RSL $A[n, L]$ is given by [5]

$$\begin{aligned} A[n, L] &= A_p[n, L] + A_w[n] + A_v[n, L] \\ &\quad + A_0[L] + r[n] + q[n] \text{ dB} \\ n &= 1, \ldots, N. \end{aligned} \tag{1}$$

We take a set of $n = 1, \ldots, N$ samples per each ML, where:

1) $L$—link length;
2) $A_p[n, L]$—path-integrated precipitation attenuation;
3) $A_v[n, L]$—other-than-rain-induced attenuation, resulting primarily from the atmospheric water vapor [37];
4) $A_0[L]$—free-space propagation loss;
5) $A_w[n]$—wet/moist antenna attenuation;
6) $q[n]$—quantization noise;
7) $r[n]$—white noise.

We note that $A_w[n]$ is independent of the link length as opposed to $A_p[n, L]$ and $A_v[n, L]$ being dependent of path length and are considered here as channel interferences.

In cellular backhaul transmission systems, the RSL is typically quantized. For simplicity, we approximate the quantization effect using additive quantization noise $q[n]$. It is modeled as an additive uniformly distributed random process with variance $\frac{\Delta^2}{12}$, where $\Delta$ is the quantization interval. This approximation is valid for $A_p[n, L]$, $A_w[n]$ and $A_v[n, L]$ as long as their dispersion is higher than the quantization interval [5]. $r[n]$ is a measurement noise at the ML receiver, and is assumed to be an additive Gaussian noise. Since the latter is added at the ML receiver, it does not dependent on the link length.

In this study, we assume that no precipitation was present during the detection interval $N$, i.e., $A_p[n, L] = 0$. This assumption was validated using rainfall data taken from the Israeli Meteorological Service (IMS). However, we note that one can use the methods suggested in [38] or [8] for identifying dry periods (when no rain occurred). It is important to note that each link comprises a transmitter and receiver which are deployed at different spatial locations.

The idea of detecting moist antenna perturbations using ML lies on the principle that the attenuation is derived only due to the water film found on the microwave antenna itself and thus it can be determined whether attenuation drop observed simultaneously by multiple links, found in the same observed region, is independent of link length. We assume here homogeneity of the water vapor and dew in the observed field. Namely, all ML in the area examined are assumed to be affected by the same moist antenna-induced attenuation and by the same water vapor effect, while the latter is being proportional to the link length. The assumption, then, is that on days when dew existed, it simultaneously wet all of the microwave antennas in the observed region. In reality, it is possible, e.g., that only one of the two antennas that comprise the link was wet, but if attenuation was detected on the link, the assumption is that the wetting was simultaneous at both antennas. There has not

been much research investigating the spatial distribution of dew, however, recent work by Rowlandson [30] shows that over an area of 1 km$^2$, dew was observed simultaneously by different dew gauges located several hundreds of meters apart, and over separate dew events. In order to justify the assumption of the simultaneous occurrence of dew in this research, we adopted a conservative definition of a dew event. An event was considered dewy during times when all five meteorological stations measured RH of at least 90% and the LWS identified dew.

Under these assumptions, the attenuation model (1) of the $i$th ML from a set of $M$ links reduces to

$$A_i[n,L] = A_w[n] + L_i \cdot A_v[n] + A_{0i}[L] + r_i[n] + q_i[n] \text{ dB}$$
$$n = 1,\ldots,N,\ i = 1,\ldots,M. \quad (2)$$

Our goal is to decide whether moist antenna attenuation, ascribed to dew, is present or is it only the water vapor induced attenuation which is observed. Therefore, the attenuation model (2) can be transformed into a binary hypothesis test aimed for detecting the moist antenna losses

$$\mathcal{H}_0:\ A_i[n,L] = L_i \cdot A_v[n] + A_{0i}[L] + r_i[n] + q_i[n]$$
$$\mathcal{H}_1:\ A_i[n,L] = A_w[n] + L_i \cdot A_v[n] + A_{0i}[L] + r_i[n] + q_i[n]$$
$$n = 1,\ldots,N,\ i = 1,\ldots,M. \quad (3)$$

In typical conditions, water vapor is present in the atmosphere with different concentrations at different altitudes. Those concentrations vary with time and space; however, spatial variations are neglected here. $\mathcal{H}_0$ is, therefore, defined as the null hypothesis and is ascribed to the attenuation fluctuations induced by variations in the atmospheric humidity. $\mathcal{H}_1$ is defined as the moist antenna attenuation hypothesis.

Typically, dew is a phenomenon that is present for at least a few hours after emerging while the absolute humidity characteristically varies more slowly over time [33]. Therefore, under these assumptions, we consider their attenuations $A_w[n]$ and $A_v[n]$ as constant transient signals of unknown arrival times $n_w$ and $n_v$ and of unknown durations $\tau_w$ and $\tau_v$, respectively.

In our problem, we assume that the base-line attenuation of each link $i$ is caused by free-space propagation loss together with the absolute humidity attenuation that exists in the atmosphere. In dewy nights, the RH typically exceeds the threshold of 85% and therefore excess water-vapor-induced attenuation is expected. In Fig. 1, we exemplify the water vapor attenuation as a function of frequency [39] for a typical dry summer afternoon and dewy summer night in Israel [33]. The gray curve denotes the water vapor attenuation, in typical late afternoon conditions, where the RH is about 60% and the temperature is 25 °C. The black curve is the water vapor attenuation exemplifying early morning conditions where the RH is about 90% and the temperature is about 18 °C. The difference between the black and gray curves is denoted by the dashed curve signifying the additional water vapor induced attenuation $\Delta A_v[n]$, created due to the typical differences between the early morning humidity and that of the late afternoon. The typical water vapor attenuation during the late afternoon, together with the unknown zero level attenuation $A_{0i}[L]$ are defined as an unknown mean defined as the base-line attenuation for each link $\mu_i$.

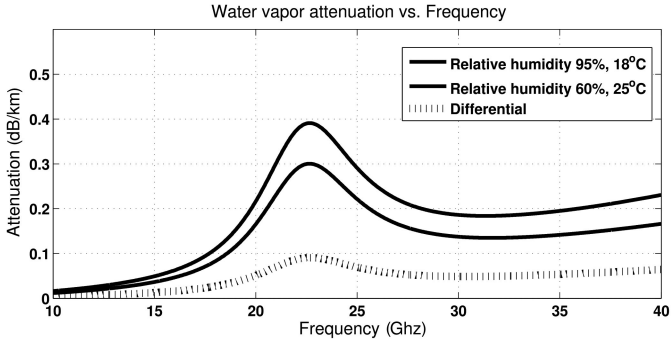


Fig. 1. Water vapor attenuation versus frequency in a typical dewy summer night in Israel. The gray curve is the water vapor attenuation, in the late afternoon, and the black curve is the water vapor attenuation, in early morning. The dashed curve is the differential water vapor attenuation. The meteorological data are based on [33] and on measurements from meteorological stations in the observed region.

In each link $i$, we model the noise measurement $r_i[n]$ and the quantization noise $q_i[n]$ by an additive white Gaussian noise (AWGN) $w_i[n]$ of unknown variance $\sigma^2$, meaning that we only use the second-order statistics of the real noise. This substitution leads to suboptimal parameter estimation, in the estimation step of the GLRT solution. In Section IV, we discuss and demonstrate the effects of this assumption on the detection performance. Additionally, we assume that the noise processes at the different sensors are independent and identically distributed (IID).

Notably, the binary hypothesis testing problem (3) is a specific problem of detecting an unknown deterministic transient signal $A_w[n]$ embedded within the interference signal. The difference between the two signals is that the moist antenna attenuation signal $A_w[n]$ affects all ML identically, while the interference signal (additional water vapor attenuation signal) affects each link proportionally to its length $L_i$.

Finally, the binary hypothesis testing problem is reduced to

$$\mathcal{H}_0:\ A_i[n,L] = L_i \cdot \Delta A_v[n\,;\,\tau_v\,,n_v] + \mu_i + w_i[n]$$
$$\mathcal{H}_1:\ A_i[n,L] = A_w[n\,;\,\tau_w\,,n_w]$$
$$+ L_i \cdot \Delta A_v[n\,;\,\tau_v\,,n_v] + \mu_i + w_i[n]$$
$$n = 1,\ldots,N,\ i = 1,\ldots,M. \quad (4)$$

Note that under each hypothesis $\mathcal{H}_0$ and $\mathcal{H}_1$, there are unknown parameters. Under $\mathcal{H}_0$, we define the $(M+4)$ dimensional vector of unknown parameters as $\underline{\theta}_0 \triangleq [\Delta A_v, n_v, \tau_v, \underline{\mu}^T, \sigma^2]^T$, whereas under $\mathcal{H}_1$, the $(M+7)$ dimensional vector of unknown parameters is defined as $\underline{\theta}_1 \triangleq [A_w, n_w, \tau_w, \Delta A_v, n_v, \tau_v, \underline{\mu}^T, \sigma^2]^T$. In (4), $A_w$ is the unknown constant moist antenna attenuation and $\Delta A_v$ is the unknown constant additional water vapor attenuation per unit of link length. The signal loss is a negative quantity and thus $A_w < 0$ and $\Delta A_v < 0$. One can note that $A_w, n_w$, and $\tau_w$ are the unknown parameters of the desired signal, while $\Delta A_v, n_v$, and $\tau_v$ are the unknown parameters of the interference signal. $\underline{\mu} \triangleq [\mu_1,\ldots,\mu_M]^T$ is $(M \times 1)$ vector consisting of the $M$ unknown measurement means (base-line attenuations).

### B. Method

In our detection problem, no prior information concerning the probabilities of the various hypotheses exists, and we can see that the pdf for each assumed hypothesis is not completely known. The uncertainty is expressed by including unknown non random parameters in the pdf. In such a case, when no uniformly most powerful (UMP) test [40] exists, the GLRT is commonly used to provide a solution [36]. The ln version of the GLRT for the binary hypothesis testing model (4) is of the form

$$L_G(\underline{X}) = \ln\left(\frac{P(\underline{X}\,;\,\hat{\underline{\theta}}_1,\,\mathcal{H}_1)}{P(\underline{X}\,;\,\hat{\underline{\theta}}_0,\,\mathcal{H}_0)}\right) \underset{\mathcal{H}_0}{\overset{\mathcal{H}_1}{\gtrless}} \gamma \tag{5}$$

where $P(\underline{X}\,;\,\underline{\theta}_1\,,\,\mathcal{H}_1)$ is the pdf of the received signal $\underline{X} \triangleq [A_1[1,L_1],\ldots,A_1[N,L_1],\ldots,A_M[1,L_M],\ldots,A_M[N,L_M]]^T$ under $\mathcal{H}_1$ with the unknown parameters vector $\underline{\theta}_1$, while $P(\underline{X}\,;\,\underline{\theta}_0\,,\,\mathcal{H}_0)$ is its pdf under $\mathcal{H}_0$ with the unknown parameters vector $\underline{\theta}_0$. $\hat{\underline{\theta}}_1$ is the maximum likelihood estimates (MLEs) [41] of $\underline{\theta}$ assuming $\mathcal{H}_1$ is true [maximizes $P(\underline{X}\,;\,\underline{\theta}_1\,,\,\mathcal{H}_1)$], and $\hat{\underline{\theta}}_0$ is the the MLE of $\underline{\theta}$ assuming $\mathcal{H}_0$ is true (maximizes $P(\underline{X}\,;\,\underline{\theta}_0\,,\,\mathcal{H}_0)$).

While there is no optimality associated with the GLRT, in some cases, it can be shown that the GLRT is asymptotically optimal, in the invariant sense [42], and in practice, it appears to acquire satisfying solutions. This test, in addition to signal detection, also provides information about the unknown parameters since the first step in computing (5) is to find the MLEs under each hypothesis.

Let us begin with evaluating the MLEs under each hypothesis. The MLE of $\underline{\theta}_0$ under $\mathcal{H}_0$ is found by maximizing the log likelihood function $L(\underline{X};\,\underline{\theta}_0)$

$$\begin{aligned}&\max_{\underline{\theta}_0}\{L(\underline{X}\,;\,\underline{\theta}_0)\}\\ &= \max_{\Delta A_v, n_v, \tau_v, \underline{\mu}, \sigma^2}\left\{-\frac{MN}{2}\ln\left(2\pi\sigma^2\right)\right.\\ &\left.-\sum_{i=1}^{M}\left(\frac{\|\underline{x}_i - L_i\cdot\Delta A_v\cdot h_v(n_v,\tau_v) - \mu_i\cdot\underline{1}\|^2}{2\sigma^2}\right)\right\}\end{aligned} \tag{6}$$

where $\underline{x}_i \triangleq [A_i[1,L_i],\ldots,A_i[N,L_i]]^T$, $\underline{1}_{N\times 1} \triangleq [1,\ldots,1]^T$, $h_v(n_v,\tau_v)$ is an $(N\times 1)$ vector, $h_{v\,n}\in\{0,1\}$, and $\|\underline{a}\|^2 \triangleq \underline{a}^T\cdot\underline{a}$.

*Theorem 1:* The MLEs of $\Delta A_v$ , $n_v$ , $\underline{\mu}$, and $\sigma^2$, which maximize (6), when the duration of the signal $\tau_v$ is fixed, and under the constraint that $\Delta\hat{A}_v \le 0$, are given by

1) $\hat{n}_v = \min_{n_v}\left\{\sum_{n=n_v}^{n_v+\tau_v-1} x_s[n]\right\}$, where $x_s[n] \triangleq \frac{1}{\left(\sum_{j=1}^{M} L_j^2\right)}$ $\sum_{i=1}^{M}(L_i\cdot x_i[n])$;
2) $\Delta\hat{A}_v = \frac{1}{\tau_v}\sum_{n=\hat{n}_v}^{\hat{n}_v+\tau_v-1} x_s[n] - \frac{1}{(N-\tau_v)}\sum_{n\notin[\hat{n}_v,\hat{n}_v+\tau_v-1]} x_s[n]$;
3) $\hat{\mu}_i = \frac{1}{N}\left(\sum_{n=1}^{N} x_i[n] - L_i\cdot\Delta\hat{A}_v\cdot\tau_v\right)$, $i=1,\ldots,M$;
4) $\hat{\sigma}^2 = \frac{1}{NM}\sum_{i=1}^{M}\|\left(\underline{x}_i - L_i\cdot\Delta\hat{A}_v\cdot h(\hat{n}_v,\tau_v) - \hat{\mu}_i\cdot\underline{1}\right)\|^2$.

*Proof:* The proof is given in Appendix A.

Bearing in mind the above, the MLE of $n_v$ under the constraint $\Delta\hat{A}_v \le 0$ from $M$ sensors is simply weighted summing their measurements, and looking for the initiating sample (time of arrival) where a time window of the sum with duration $\tau_v$ is minimal. The MLE of $\Delta A_v$, $\underline{\mu}$, and $\sigma^2$, when inserting the MLE of $n_v$, are found by the regular solution of a linear model Gaussian problem.

The MLE of $\tau_v$ is found by inserting $\Delta\hat{A}_v$ , $\hat{n}_v$ , $\hat{\underline{\mu}}$, and $\hat{\sigma}^2$ (Theorem 1) into (6), and searching for the value of $\tau_v \in [\tau_1,\tau_2]$ that achieves the maximum value, where $\tau_1$ and $\tau_2$ are *a priori* thresholds of the duration of the signal $\Delta A_v$, meaning that the minimum duration of the signal is $\tau_1$ and the maximum duration is $\tau_2$

$$\hat{\tau}_v = \min_{\tau_v\,\in\,[\tau_1,\tau_2]}\left\{\ln\left(2\pi\hat{\sigma}^2\right)\right\}. \tag{7}$$

Note that we assume in (7) that the observation interval $N$ is longer than the duration of the additional water vapor attenuation signal $N > \tau_2$, i.e., we choose observation interval that lasts longer than a typical water vapor phenomena (reasonable under typical Israeli weather conditions, as aforementioned [33]).

The MLE of $\theta_1$ under $\mathcal{H}_1$ is found by maximizing the log likelihood function $L(\underline{X}\,;\,\underline{\theta}_1)$

$$\begin{aligned}&\max_{\underline{\theta}_1}\{L(\underline{X}\,;\,\underline{\theta}_1)\}\\ &= \max_{\underline{\theta}_1}\left\{-\frac{MN}{2}\ln\left(2\pi\sigma^2\right) - \frac{1}{2\sigma^2}\sum_{i=1}^{M}(\|\underline{x}_i - A_w\cdot h_w(n_w,\tau_w)\right.\\ &\left.-L_i\cdot\Delta A_v\cdot h_v(n_v,\tau_v) - \mu_i\cdot\underline{1}\|^2)\right\}\end{aligned} \tag{8}$$

where $h_w(n_w,\tau_w)$, as $h_v(n_v,\tau_v)$, is an $(N\times 1)$ vector, $h_{w\,n}\in\{0,1\}$.

The appearance of dew is highly dependent on the atmospheric RH. The threshold RH above which dew is likely to emerge can be assumed to be 85% [33]. Due to this dependence we assume that moist antenna attenuation, which is caused by dew, can appear only during high RH conditions, i.e., during times when additional water-vapor-induced attenuation is expected to appear. This assumption is reasonable, since the ascension of humidity induces additional water vapor attenuation, and when it exceeds approximately the threshold of 85%, moist antenna attenuation is likely to emerge. Mathematically, that means that under $\mathcal{H}_1$ we assume that $n_w \ge n_v$ and $n_w + \tau_w < n_v + \tau_v$, i.e., the desired signal $A_w[n\,;\,n_w,\tau_w]$ appears only during the interference signal $\Delta A_v[n\,;n_v,\tau_v]$. We use this assumption to facilitate the MLE solution under $\mathcal{H}_1$ (8).

The MLE solution for $\theta_1$ is a 4-D search over $n_w$ , $\tau_w$ , $n_v$, and $\tau_v$, and for any combination of these four parameters, we deal with a quadratic optimization problem under constraints ($\hat{A}_w \le 0$ , $\Delta\hat{A}_v \le 0$). Note that the MLEs of $\Delta A_v, n_v, \tau_v, \underline{\mu}$, and $\sigma^2$ are different under each hypothesis.

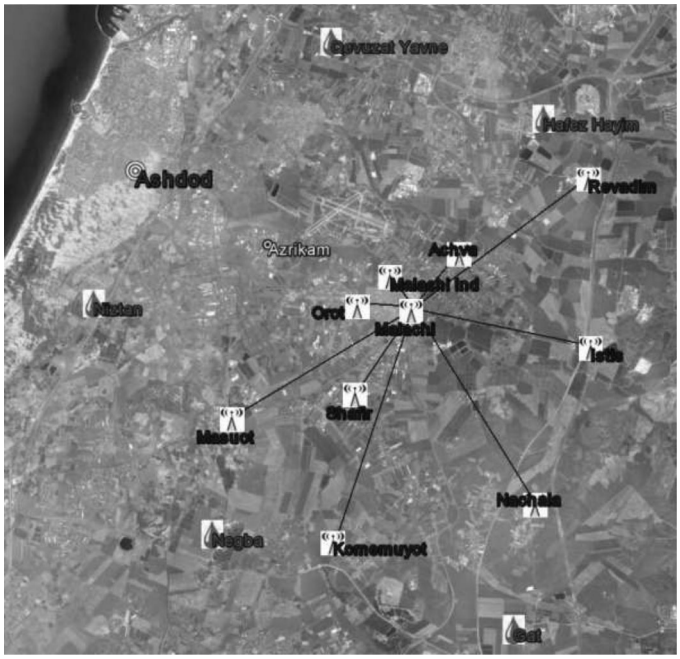


F2:1 Fig. 2. Map of MLs (lines), meteorological stations (drop signs), and LWS
F2:2 (circle sign).

Finally, we substitute the estimates, $\hat{\underline{\theta}}_1$ and $\hat{\underline{\theta}}_0$, into (5) in order to get the GLRT test

$$L_G(\underline{X}) = -\frac{MN}{2}\ln\left(2\pi\hat{\sigma}_1^2\right) - \frac{MN}{2} + \frac{MN}{2}\ln\left(2\pi\hat{\sigma}_0^2\right) + \frac{MN}{2} = \frac{MN}{2}\ln\left(\frac{\hat{\sigma}_0^2}{\hat{\sigma}_1^2}\right) \underset{\mathcal{H}_0}{\overset{\mathcal{H}_1}{\gtrless}} \gamma \tag{9}$$

where $\hat{\sigma}_1^2$ is the estimation of $\sigma^2$ under $\mathcal{H}_1$ and $\hat{\sigma}_0^2$ is under $\mathcal{H}_0$. The threshold $\gamma$ is set to determine the desired false alarm rate using standard techniques [34]. In Section IV, we present the experimental ROC obtained.

## III. Experimental Setup and Model Assumptions

Commercial MLs operate at frequencies of tens of GHz, at ground level altitudes. The RSL measurements are quantized in steps of several decibels down to 0.1 dB, typically. Built-in facilities enable RSL recording at various temporal resolutions, depending on the type of the equipment (typically between once per minute and once per day).

In this study, a microwave system comprised fixed terrestrial line-of-sight links, employed for data transmission between cellular base stations was used. We focused on 18 ML spread across central Israel as described in Fig. 2. The technical specifications of the ML used are denoted in Table I. Each link provides RSL records in 1 min intervals with a quantization level of 1 dB. As can be seen in Table I, four different frequencies were used, however, since the algorithm aims at detection purposes only (i.e., not estimation of the different parameters) the effect of frequency dependence on attenuation was neglected. This action can be justified by the following reasons: the algorithm estimates the excess water vapor attenuation.

TABLE I T1:1
Microwave Links T1:2

| ML name | Frequency (GHz) | Length (km) |
|---|---|---|
| K. Malachi—Orot | 18.82/17.81 | 1.9 |
| K. Malachi—Achva | 23.75/22.075 | 2.6 |
| K. Malachi—Revadim | 18.82/17.81 | 8 |
| K. Malachi—Nachala | 18.82/17.81 | 8 |
| K. Malachi—M. Izhak | 18.958/17.948 | 7.44 |
| K. Malachi—Komemiyot | 18.958/17.948 | 8.5 |
| K. Malachi—Istis | 18.82/17.81 | 6.5 |
| K. Malachi—K. Malachi Ind | 23.275/22.075 | 1.4 |
| K. Malachi—Shafir | 23.275/22.075 | 3.5 |

However, as depicted in Fig. 1, the differential water vapor attenuation is weakly dependent on frequency. The algorithm also calculates the attenuation due to antenna wetting which is known to be weakly dependent on frequency, particularly at the given relatively narrow frequency range [43]. In Section IV, we verify this assumption.

In order to quantify and validate the results obtained using the proposed technique, we used the LWS for detecting the dewy events. The LWS is located in the vicinity of the microwave system as illustrated in Fig. 2. In addition, RH measurements from five meteorological stations, as shown in Fig. 2 were utilized. The RH measurements in conjunction with the LWS detections determined which of the events was dewy. An event was considered dewy during times when all five meteorological stations measured RH of at least 90% and the LWS identified dew. Under these conditions, these measurements were then compared to the microwave system wet antenna detections acquired using the proposed methodology. Notably, some disparities are expected between the different ways of measuring a moist event (i.e., dew versus wet antenna) as discussed in the conclusions. The justification for the comparison made between the two observations arises from the fact that both phenomena, dew and moist antenna, appear whenever the condensation rate exceeds evaporation rate during times of high atmospheric RH. As a consequence, the detection of moist antenna phenomenon can point to the presence of dew, as will be exemplified in the next section. It is important to note that moist antenna phenomenon cannot be considered straightforwardly as dew, as will be discussed in the conclusion.

## IV. Results

We applied the GLRT (9) to RSL measurements which were taken from 40 nights (events) during the months of February to July 2010. Based on measurements made with meteorological instruments, 20 events were detected as dewy ones, and 20 were identified as dry, i.e., when no dew was observed by the LWS (at RH $< 90\%$). The duration of each event (namely, the observation interval $N$) was chosen to be 14 h ($N = 840$ samples), i.e., long enough to accommodate the variations within the atmospheric phenomena observed (dew, water vapor) [33]. Under the no moist antenna hypothesis $\mathcal{H}_0$, we assume that the

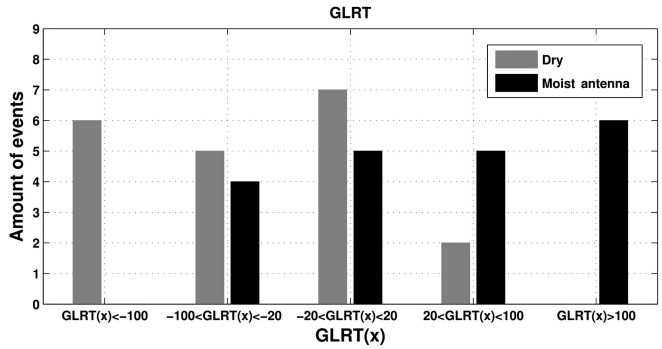


F3:1 Fig. 3. GLRT plane. Black bars are events that were considered as moist by
F3:2 the meteorological instruments, whereas the gray bars are events that were
F3:3 considered as just water vapor changes.

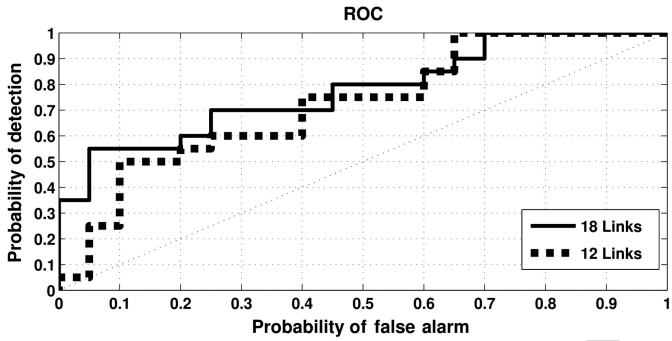


F4:1 Fig. 4. Probability of detection versus the probability of false alarm for the
F4:2 detection of moist antenna events, using the GLRT.

duration of the additional water vapor attenuation can receive any value for $\tau_v$ between 2 and 10 h, and under the moist antenna hypothesis $\mathcal{H}_1$, as explained in Section II, we add the assumption that $n_w \geq n_v$ and $n_w + \tau_w < n_v + \tau_v$.

The detection performance is presented by an ROC curve. The ROC illustrates the probability of detection $P_D$ (i.e., the algorithm indicated a moist antenna signal and in reality it was present) versus the probability of false alarm $P_{FA}$ (i.e., the algorithm indicated a moist antenna signal, but in reality it was not present).

Fig. 3 presents the GLRT's derived from measurements of 18 ML for the 40 events studied. The x-axis presents the GLRT plane, while the y-axis indicates the the number of events. The black bars are the events that were considered as moist by the RH measurements, from the five meteorological stations, and by the LWS identification. The gray bars are the events that were considered as just water vapor changes. It can be seen that there is a distinction between the two hypotheses, with moderate significance though. The ROC, in Fig. 4, was derived from the results depicted in Fig. 3. The figure presents the ROC of the GLRT based on measurements from 18 ML (black curve). For comparison, the ROC of the GLRT based on 12 ML (gray-dashed curve) is also given (the 12 ML were chosen to be the ones that operate at frequencies of around 17 and 18 GHz).

Table II details the estimation results of the GLRT for the additional water vapor attenuation and the moist antenna attenuation, based on five representative dewy events. As described previously in Section I, there is a relatively small amount of research dealing with monitoring other-than-precipitation

TABLE II T2:1
ESTIMATION RESULTS T2:2

| Date | $\Delta\hat{A}_v\left(\frac{\text{dB}}{\text{km}}\right)$ | $\hat{A}_w$ (dB) |
|---|---|---|
| 19.2.10–20.2.10 | $-0.028$ | $-0.37$ |
| 26.3.10–27.3.10 | $-0.069$ | $-0.67$ |
| 6.4.10–7.4.10 | $-0.029$ | $-0.52$ |
| 28.5.10–29.5.10 | $-0.04$ | $-0.15$ |
| 31.5.10–1.6.10 | $-0.027$ | $-0.74$ |

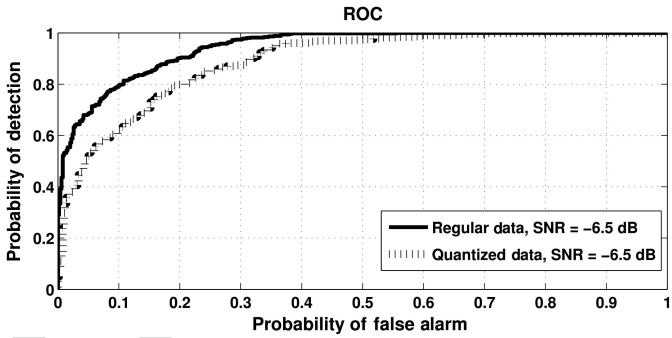


Fig. 5. Probability of detection versus the probability of false alarm for the F5:1
GLRT using quantized data and un-quantized data. In all the events, the true F5:2
signal was $A_w = 0.15$, the true interference signal was $A_v = 0.05$, and the F5:3
true variance of the Gaussian noise was $\sigma^2 = 0.1$. F5:4

phenomena using measurements from ML. As a consequence, currently, there is a limited capacity to compare and verify results in this area. However, it is notable that the moist antenna estimation results are of the same order of magnitude as those found by Hening and Stanton [17]. They found that the attenuation caused by dew at 20 GHz is approximately 0.5 dB. Moreover, the additional water vapor attenuation results obtained are of the same order comparing to the excessive water vapor curve depicted in Fig. 1, when focusing on the relevant frequencies.

The quantization noise is also a factor that may strongly affect the detection performance. Notably, the magnitude of the water vapor and moist antenna excess attenuation are of the same order as that of the quantization interval. Hence, the algorithm-based estimates are impaired. In order to examine this effect, a comparison between the GLRT ROCs derived for quantized and un-quantized data was produced by a computer simulation, as presented in Fig. 5. The GLRT (9) was applied on 1 dB quantized data and un-quantized data for 1000 events simulated (500—moist antenna events, 500—water vapor changes events) using 4 links ($M = 4$). The true values chosen of $A_w$ and $A_v$, are based on values found in literature.

## V. CONCLUSION

The results point to the potential of detecting dewy episodes using already existing commercial ML. The results (Figs. 3 and 4) demonstrate that adding links improves performance of the detection algorithm. The 18 ML-based curve (black) where frequencies of 17–23 GHz were used achieved better results than the 12 ML-based curve (gray) where frequencies of only

17–18 GHz were used. In this case, the amount of links had a greater impact on the detection performance than the accuracy of the model. Therefore, it is reasonable to assume that the attenuation due to excessive water vapor and moist antenna on the ML is weakly dependent on frequency.

Figs. 3 and 4 present a moderate distinction between the two hypotheses. While further investigation is required concerning this issue, we can point to the following aspects that would affect these results: first, as mentioned, moist antenna phenomena cannot straightforwardly be considered as dew. Therefore, since we validate the performance of the GLRT algorithm by the LWS, which identifies dew, there is a possibility that even though the sensor identified the event as dewy, a moist layer did not accumulate on the antenna surface in a specific event. Having said that, it is possible then that the four negative events (black bar) observed in Fig. 3 are an example of such cases. That is, these events were detected as dewy by the LWS while the GLRT algorithm classified them as no moist antenna events.

Fig. 5 points to a significant gap between the ROC curve of quantized data and that of un-quantized data, for SNR $=$ $-6.5$ dB $\left(\text{SNR} \triangleq 10\log\left(\frac{A_w^2}{\sigma^2}\right)\right)$. However, it should be noted that more sensitive microwave systems exists with digital quantization of, e.g., 0.1 dB [11], [14]. Hence, it is expected that applying the algorithm on such RSL data will improve accuracy when compared to microwave systems with coarser sensitivity (as the system utilized in this study).

While a principle feasibility has been demonstrated, additional experimental and modeling research are required. The contribution of transmission loss due to atmospheric phenomena (e.g., fog) and due to the wettings of the antennas, as well as the effect of antenna elevation (ranging from several meters to several tens of meters) off the surface should be studied. Further experimental verification should also take into account the inherent uncertainty of reference data, including technical limitations of dew meters, difference in wetting properties of materials, in particular: the microwave radomes are artificial materials with different thermal properties comparing to those of soil or vegetation pallets. Moreover, the difference of orientation of the wetting surfaces, microwave radomes are vertical surfaces while typical dew meters are horizontal surfaces.

Since dew has a cardinal part in various ecological processes, the numerous microwave antennas, acting as a dew detector unit, have the potential to shed light on the role of this phenomenon in the local and global ecosystems.

## APPENDIX A
## PROOF OF THEOREM 1

Let us consider first the case of $M = 1$. Thus, when using one sensor and when the duration of the signal $\tau_v$ is fixed, (6) reduces to

$$\max_{\Delta A_v, n_v, \mu, \sigma^2} \left\{ -\frac{N}{2}\ln\left(2\pi\sigma^2\right) - \left( \frac{\|\underline{x} - L\cdot\Delta A_v \cdot h_v(n_v,\tau_v) - \mu\cdot\underline{1}\|^2}{2\sigma^2} \right) \right\} \tag{A1}$$

The MLE of $\sigma^2$, when $\Delta A_v$ , $n_v$, and $\mu$ are fixed, is given by

$$\hat{\sigma}^2 = \frac{1}{N}\left(\|\underline{x} - L\cdot\Delta A_v \cdot h_v(n_v,\tau_v) - \mu\cdot\underline{1}\|^2\right) \tag{A2}$$

substituting (A2) into (A1) yields

$$\min_{\Delta A_v, n_v, \mu} \left\{ \left(\|\underline{x} - L\cdot\Delta A_v \cdot h_v(n_v,\tau_v) - \mu\cdot\underline{1}\|^2\right) \right\}. \tag{A3}$$

The MLE of $\mu$, when $A_v$ and $n_v$ are fixed, is given by

$$\begin{aligned}\hat{\mu} &= \left(\underline{1}^T\cdot\underline{1}\right)^{-1}\cdot\underline{1}^T\cdot\left(\underline{x} - L\cdot\Delta A_v\cdot h_v(n_v,\tau_v)\right) \\ &= \frac{1}{N}\left(\sum_{n=1}^{N} x[n] - L\cdot\tau_v\cdot\Delta A_v\right)\end{aligned} \tag{A4}$$

substituting (A4) into (A3) and simplifying yields

$$\begin{aligned}\min_{\Delta A_v, n_v} \big\{ &\underline{x}^T\cdot Q\cdot\underline{x} - 2\cdot L\cdot\Delta A_v\cdot\underline{x}^T\cdot Q\cdot h_v(n_v,\tau_v) \\ &+ L^2\cdot(\Delta A_v)^2\cdot h_v(n_v,\tau_v)^T\cdot Q\cdot h_v(n_v,\tau_v)\big\}\end{aligned} \tag{A5}$$

where $Q \triangleq \left(I_{N\times N} - \frac{1}{N}\cdot\underline{1}\cdot\underline{1}^T\right)$ is a projection matrix.

Note that the expression $\underline{x}^T\cdot Q\cdot\underline{x}$ in (A5) is independent of $A_v$ or $n_v$ and therefore (A5) reduces to

$$\begin{aligned}\min_{\Delta A_v, n_v} \big\{ &-2\cdot\Delta A_v\cdot(\underline{x}^T/L)\cdot Q\cdot h_v(n_v,\tau_v) \\ &+ (\Delta A_v)^2\cdot h_v(n_v,\tau_v)^T\cdot Q\cdot h_v(n_v,\tau_v)\big\}\end{aligned} \tag{A6}$$

The MLE of $\Delta A_v$, when $n_v$ is fixed, is given by

$$\begin{aligned}\Delta\hat{A}_v &= \frac{1}{L}\left(h_v(n_v,\tau_v)^T Q h_v(n_v,\tau_v)\right)^{-1}\cdot h_v(n_v,\tau_v)^T Q\underline{x} \\ &= \frac{1}{L}\left(\frac{1}{\tau_v}\sum_{n=n_v}^{n_v+\tau_v-1} x[n] - \frac{1}{(N-\tau_v)}\sum_{n\notin[n_v,n_v+\tau_v-1]} x[n]\right)\end{aligned} \tag{A7}$$

Note that

$$h_v(n_v,\tau_v)^T\cdot Q\cdot h_v(n_v,\tau_v) = \tau_v - \frac{\tau_v^2}{N} \tag{A8}$$

using (A8) and rearranging (A7) yields

$$\Delta\hat{A}_v\cdot\left(\tau_v - \frac{\tau_v^2}{N}\right) = \left(\underline{x}^T/L\right)\cdot Q\cdot h_v(n_v,\tau_v) \tag{A9}$$

substituting (A8) and (A9) into (A6) yields

$$\max_{n_v}\left\{\left(\tau_v - \frac{\tau_v^2}{N}\right)\cdot\left(L\cdot\Delta\hat{A}_v\right)^2\right\} \tag{A10}$$

We use the prior information under $\mathcal{H}_0$; hence, the expression $\left(\tau_v - \frac{\tau_v^2}{N}\right)$ is positive $\forall\,\tau_v \in [\tau_1,\tau_2]$, where $\tau_2 < N$, so (A10) becomes

$$\max_{n_v}\left\{\left(L\cdot\Delta\hat{A}_v\right)^2\right\} = \max_{n_v}\left\{\left(\frac{1}{\tau_v}\sum_{n=n_v}^{n_v+\tau_v-1} x[n] - \frac{1}{(N-\tau_v)}\sum_{n\notin[n_v,n_v+\tau_v-1]} x[n]\right)^2\right\} \tag{A11}$$

Using the fact that $\Delta\hat{A}_v \leq 0$, (A11) reduces to

$$\min_{n_v}\left\{\frac{1}{\tau_v}\sum_{n=n_v}^{n_v+\tau_v-1}x[n]-\frac{1}{(N-\tau_v)}\sum_{n\notin[n_v,n_v+\tau_v-1]}x[n]\right\}$$

and therefore the MLE of $n_v$ is given by

$$\hat{n}_v=\min_{n_v}\left\{\sum_{n=n_v}^{n_v+\tau_v-1}x[n]\right\}. \tag{A12}$$

For the MLE of $\Delta A_v$, we insert $\hat{n}_v$ (A12) into (A7) and for the MLE of $\mu$, we insert $\hat{n}_v$ (A12) and $\Delta\hat{A}_v$ (A7) into (A4). The same process happens with the MLE of $\sigma^2$, where we insert $\hat{n}_v$, $\Delta\hat{A}_v$ and $\hat{\mu}$ into (A2).

Finally, we show how the case of $M>1$ is reduced to the case of $M=1$, when the measurements vector is $x_s[n]$. First, we find the MLE of $\sigma^2$ and for each sensor $i$ the MLE of $\mu_i$, when $\Delta A_v$ and $n_v$ are fixed, as in (A2) and (A4)

$$\hat{\sigma}^2=\frac{1}{NM}\sum_{i=1}^{M}\|\left(\underline{x}_i-L_i\cdot\Delta A_v\cdot h_v(n_v,\tau_v)-\mu_i\cdot\underline{1}\right)\|^2 \tag{A13}$$

$$\hat{\mu}_i=\frac{1}{N}\left(\sum_{n=1}^{N}x_i[n]-L_i\cdot\tau_v\cdot\Delta A_v\right),\ i=1,\ldots,M. \tag{A14}$$

Substituting (A13) and (A14) into (6) yields

$$\begin{aligned}&\min_{\Delta A_v,n_v}\left\{\sum_{i=1}^{M}\left(\|Q\underline{x}_i-L_i\cdot\Delta A_v\cdot Qh_v(n_v,\tau_v)\|^2\right)\right\}\\&=\min_{\Delta A_v,n_v}\left\{-2\cdot\Delta A_v\sum_{i=1}^{M}\left(L_i\cdot\underline{x}_i^T\right)Qh_v(n_v,\tau_v)\right.\\&\left.+\sum_{i=1}^{M}L_i^2\cdot(\Delta A_v)^2\cdot h_v(n_v,\tau_v)^TQh_v(n_v,\tau_v)\right\}\\&=\min_{\Delta A_v,n_v}\left\{-2\cdot\Delta A_v\frac{\sum_{i=1}^{M}\left(L_i\underline{x}_i^T\right)}{\sum_{j=1}^{M}L_j^2}Qh_v(n_v,\tau_v)\right.\\&\left.+(\Delta A_v)^2h_v(n_v,\tau_v)^TQh_v(n_v,\tau_v)\right\}\end{aligned} \tag{A15}$$

We can see that (A15) is the same optimization problem as (A6), except for the replacement of $\underline{x}^T$ by $\sum_{i=1}^{M}\left(L_i\cdot\underline{x}_i^T\right)$ and $L$ by $\sum_{j=1}^{M}L_i^2$, i.e., we replaced $\frac{\underline{x}^T}{L}$ by $\underline{x}_s^T$. Hence, the MLE of $\underline{\theta}_0$, which maximizes (6), is found by Theorem 1.

## ACKNOWLEDGMENT

This paper is dedicated to the newborn $Tal$, which means "dew" in Hebrew, the son of Debbie and weather expert Asaf Rayitsfeld from the IMS to whom we owe gratitude for the practical meteorological consultation. The authors are grateful to N. Dvela (Pelephone), Y. Dagan, Y. Eisenberg, E. Levi, S. Shilyan, and I. Alexandrovitz (Cellcom), H. B. Shabat, A. Shor, H. Mushvilli, and Y. Bar Asher (Orange) for providing the microwave data for our research. They also deeply thank the IMS for providing meteorological reference data. They extend special thanks to TAU research team members, for many fruitful discussion and valuable remarks: late Dr. R. Samuels, E. Heiman, Y. Liberman, O. Auslender, Y. Ostrometzky, R. Radian, and Y. Cantor.

## REFERENCES

[1] H. Messer, A. Zinevich, and P. Alpert, "Environmental monitoring by wireless communication networks," *Science*, vol. 312, no. 5774, p. 713, May 2006.

[2] H. Leijnse, R. Uijlenhoet, and J. N. M. Stricker, "Rainfall measurement using radio links from cellular communication networks," *Water Resour. Res.*, vol. 43, p. W03201, Mar. 2007.

[3] A. Zinevich, H. Messer, and P. Alpert, "Estimation of rainfall fields using commercial microwave communication networks of variable density," *Adv. Water Resour.*, vol. 31, pp. 1470–1480, Nov. 2008.

[4] A. Zinevich, H. Messer, and P. Alpert, "Frontal rainfall observation by a commercial microwave communication network," *Amer. Meteorol. Soc.*, vol. 48, pp. 1317–1334, Jul. 2009.

[5] A. Zinevich, H. Messer, and P. Alpert, "Prediction of rainfall intensity measurement errors using commercial microwave communication links," *Atmos. Meas. Techn.*, vol. 5, no. 3, pp. 1385–1402, 2010.

[6] Z. Wang, M. Schleiss, J. Jaffrain, A. Berne, and J. Rieckermann, "Using Markov switching models to infer dry and rainy periods from telecommunication microwave link signals," *Atmos. Meas. Techn.*, vol. 5, pp. 1847–1859, 2012.

[7] A. Gmeiner *et al.*, "Precipitation observation using microwave backhaul links in the alpine and pre-alpine region of southern Germany," *Hydrol. Earth Syst. Sci.*, vol. 16, no. 8, pp. 2647–2661, Aug. 2012.

[8] O. Harel and H. Messer, "Extension of the MFLRT to detect an unknown deterministic signal using multiple sensors, applied for precipitation detection," *IEEE Signal Process. Lett.*, vol. 20, no. 10, pp. 945–948, Oct. 2013.

[9] N. David, P. Alpert, and H. Messer, "The potential of cellular network infrastructures for sudden rainfall monitoring in dry climate regions," *Atmos. Res.*, vol. 131, pp. 13–21, Jan. 2013.

[10] H. Leijnse, R. Uijlenhoet, and J. N. M. Stricker, "Hydrometeorological application of microwave link: 1. Evaporation," *Water Resour. Res.*, vol. 43, p. W04416, Apr. 2007.

[11] N. David, P. Alpert, and H. Messer, "Novel method for water vapour monitoring using wireless communication networks measurements," *Atmos. Chem. Phys.*, vol. 7, pp. 2413–2418, Apr. 2009.

[12] N. David, P. Alpert, and H. Messer, Humidity Measurements Using Commercial Microwave Links, Aadvanced Trends in Wireless Communications. Croatia, Europe: InTech Publications, 2011.

[13] C. Chwala, H. Kunstmann, S. Hipp, and U. Siart, "A monostatic microwave transmission experiment for line integrated precipitation and humidity remote sensing," *Atmos. Res.*, vol. 144, pp. 57–62, Jul. 2013.

[14] N. David, P. Alpert, and H. Messer, "The potential of commercial microwave networks to monitor dense fog-feasibility study," *J. Geophys. Res. Atmos.*, vol. 180, no. 20, pp. 11750–11761, 2013.

[15] N. David, O. Sendik, H. Messer, and P. Alpert, "Cellular network infrastructure-the future of fog monitoring?," *Bull. Amer. Meteorol. Soc.*, vol. 96, no. 11, 2014, doi: 10.1175/BAMS-D-13-00292.1, in press.

[16] M. Schleiss, J. Rieckermann, and A. Berne, "Quantification and modeling of wet-antenna attenuation for commercial microwave links," *IEEE Geosci. Remote Sens. Lett.*, vol. 10, no. 5, pp. 1195–1199, Feb. 2013.

[17] R. E. Henning and J. R. Stanton, "Effects of dew on millimeter-wave propagation," *in Proc. IEEE Southeastcon Bringing Together Educ. Sci. Technol.*, Apr. 1996, pp. 684–687.

[18] AMS, *AMS Glossary of Meteorology*, 2nd ed. Boston, MA, USA: American Meteorological Society, 2000 [Online]. Available: http://amsglossary.allenpress.com/glossary/browse.

[19] A. A. Degen, A. Leeper, and M. Shachak, "The effect of slope direction and population density on water influx in a desert snail, Trochoidea seetzenii," *Funct. Ecol.*, vol. 6, pp. 160–166, 1992.

[20] M. Moffett, "An Indian ant's novel method for obtaining water," *Nat. Geogr. Res.*, vol. 1, no. 1, pp. 146–149, 1985.

[21] A. Danin, Y. Bar-Or, I. Dor, and T. Yisraeli, "The role of cyanobacteria in stabilization of sand dunes in southern Israel," *Ecol. Mediterr.*, vol. 15, pp. 55–64, 1989.

[22] O. Lange, G. Kidron, B. Budel, A. Meyer, E. Kilian, and A. Abeliovich, "Taxonomic composition and photosynthetic characteristics of the biological soil crusts covering sand dunes in the western Negev desert," *Funct. Ecol.*, vol. 6, no. 5, pp. 519–527, 1992.
[23] P. Petropoulosa, I. Gareth, P. K. Srivastavabc, and P. Ioannou-Katidisa, "An appraisal of the accuracy of operational soil moisture estimates from SMOS MIRAS using validated in situ observations acquired in a mediterranean environment," *Int. J. Remote Sens.*, vol. 35, pp. 5239–5250, Jul. 2014.
[24] Y. H. Kerr *et al.*, "The SMOS soil moisture retrieval algorithm," *IEEE Trans. Geosci. Remote Sens.*, vol. 50, no. 5, pp. 1384–1403, May 2012.
[25] A. M. Richard, D. Jeu, R. H. H. Thomas, and M. Owe, "Determination of the effect of dew on passive microwave observations from space," *Proc. SPIE Remote Sens. Agric. Ecosyst. Hydrol.*, Oct. 2005, vol. 5976, p. 597608.
[26] B. Hornbuckle, A. England, M. Anderson, and B. Viner, "The effect of free water in a maize canopy on microwave emission at 1.4 GHz." *Agric. For. Meteorol.*, vol. 138, pp. 180–191, Aug. 2006.
[27] B. Hornbuckle, A. England, and M. Anderson, "The effect of intercepted precipitation on the microwave emission of maize at 1.4 GHz," *IEEE Trans. Geosci. Remote Sens.*, vol. 45, no. 7, pp. 1988–1995, Jul. 2007.
[28] J. Du *et al.*, "Effect of dew on aircraft-based passive microwave observations over an agricultural domain," *J. Appl. Remote Sens.*, vol. 6, no. 1, pp. 063571-1–063571-10, Aug. 2012.
[29] P. C. Sentelhasa, A. D. Martab, S. Orlandinib, E. A. Santosc, T. J. Gillespiec, and M. L. Gleasond, "Suitability of relative humidity as an estimator of leaf wetness duration," *Agric. For. Meteorol.*, vol. 148, pp. 392–400, Mar. 2008.
[30] T. L. Rowlandson, "Leaf wetness: Implications for agriculture and remote sensing," Graduate Theses and Dissertations, Iowa State University, *Ames, IA, USA*, 2011.
[31] J. Ben-Asher, P. Alpert, and A. Ben-Zvi, "Dew is a major factor affecting the vegetation water use efficiency rather than a source of water in the eastern mediterranean," *Water Resour. Res.*, vol. 46, p. W10 532, 2010, doi: 10.1029/2008WR007484.
[32] M. Moro, A. Were, L. Villagarcia, Y. Canton, and F. Domingo, "Dew measurement by Eddy covariance and wetness sensor in a semiarid ecosystem of SE Spain," *J. Hydrol.*, vol. 335, pp. 295–302, Mar. 2007.
[33] Y. Golderich, *The Climate of Israel: Observation, Research and Application*. Ramat Gan, Israel: Bar-Ilan Press, 1998.
[34] S. Kay, Fundamentals of Statistical Signal Processing: Detection Theory. Englewood Cliffs, NJ, USA: Prentice-Hall, 1998.
[35] A. Overeem, H. Leijnse, and U. R, "Country-wide rainfall maps from cellular communication networks," *Proc. Nat. Acad. Sci.*, vol. 110, no. 8, pp. 2741–2745, 2013.
[36] H. Messer and M. Frisch, "Transient signal detection using prior information in the likelihood ratio test," *IEEE Trans. Signal Process.*, vol. 41, no. 6, pp. 2177–2192, Jun. 1993.
[37] D. Thomas and J. L. Frey, "The effects of the atmosphere and weather on the performance of a mm-wave communication link," *Appl. Microw. Wireless*, vol. 13, no. 1, pp. 76–80, Feb. 1997.
[38] M. Schleiss and A. Berne, "Identification of dry and rainy periods using telecommunciation microwave links," *IEEE Geosci. Remote Sens. Soc.*, vol. 7, no. 3, pp. 611–615, Jul. 2010.
[39] International Telecommunication Union (ITU), "Attenuation by atmospheric gases," ITU-Recommendations, R.I.-R. P. 676–6, 2005.
[40] L. L. Scharf, *Statistical Signal Processing*. Reading, MA, USA: Addison-Wesley, 1991.
[41] S. Kay, Fundamentals of Statistical Signal Processing: Estimation Theory. Englewood Cliffs, NJ, USA: Prentice-Hall, 1998.
[42] L. L. Scharf and B. Friedlander, "Matched subspace detectors," *IEEE Trans. Signal Process.*, vol. 42, no. 8, pp. 2146–2157, Aug. 2002.
[43] H. Leijnse, "Hydrometeorological appliction of microwave links," Ph.D. dissertation, Wageningen University, Wageningen, The Netherlands, 2007.

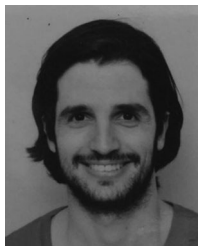

**Oz Harel** received the B.Sc. and M.Sc. (through the direct master's program) degrees in electrical engineering from the Faculty of Engineering, Tel Aviv University (TAU), Tel Aviv, Israel.

Currently, he works as Algorithm Engineer in the microwave communication industry. His research interests include statistical signal processing, remote sensing, and environmental monitoring.

**Noam David** received the B.Sc. (with distinction) and Ph.D. (through the direct doctoral track) degrees in geosciences from Tel Aviv University, Tel Aviv, Israel.

He currently holds a Postdoctoral position with the School of Civil and Environmental Engineering, Cornell University, Ithaca, NY, USA. His research interests include weather and atmospheric sciences, wave matter interaction, remote sensing, air quality, and environmental monitoring.

**Pinhas Alpert** received the Ph.D. degree in meteorology from the Hebrew University of Jerusalem, Jerusalem, Israel, in 1980.

He joined the Department of Geosciences, Tel Aviv University, Tel Aviv, Israel, in 1982, after a Postdoctorate at Harvard University, Cambridge, MA, USA. He is currently the Mikhael M. Nebenzahl and Amalia Grossberg Chair Professor of Geodynamics. He served as the Head of the Porter School of Environmental Studies, Tel-Aviv University, during 2008–2013, following 3 years as Head of the Department of Geosciences at Tel Aviv University. He established and Heads the Israel Space Agency Middle East Interactive Data Archive (ISA-MEIDA), Tel Aviv, Israel. He is a Co-Director of the GLOWA-Jordan River BMBF/MOS project to study the water vulnerability in the E. Mediterranean and served as the Israel Representative to the IPCC TAR WG1. His research interests include atmospheric dynamics, climate, numerical methods, limited area modeling, aerosol dynamics, and climate change.

**Hagit Messer** (F'00) received the Ph.D. degree in electrical engineering from Tel Aviv University (TAU), Tel Aviv, Israel.

After a Postdoctoral Fellowship with Yale University, New Haven, CT, USA, she joined the Faculty of Engineering, Tel Aviv University, in 1986, where she is a Professor of Electrical Engineering. During 2000–2003, she was on leave from TAU, serving as the Chief Scientist at the Ministry of Science. After returning to TAU, she was the Head of the Porter School of Environmental Studies (2004–2006) and the Vice President for Research and Development (2006–2008). Then, she has been the President of the Open University, and from October 2013, she serves as the Vice Chair of the Council of Higher Education, Jerusalem, Israel. She is an Expert in statistical signal processing with applications to source localization, communication and environmental monitoring. She has authored numerous journal and conference papers, and has supervised tens of graduate students.

Prof. Messer has been a member of Technical Committees of the Signal Processing Society since 1993 and on the Editorial Boards of the IEEE TRANSACTIONS ON SIGNAL PROCESSING, the IEEE SIGNAL PROCESSING LETTERS, the IEEE JOURNAL OF SELECTED TOPICS IN SIGNAL PROCESSING (J-STSP), and on the Overview Editorial Board of the Signal Processing Society journals.